

Online non-convex learning for river pollution source identification*

Wenjie Huang [†] Jing Jiang [‡] Xiao Liu [§]

May 25, 2020

Abstract

In this paper, novel gradient based online learning algorithms are developed to investigate an important environmental application: real-time river pollution source identification, which aims at estimating the released mass, the location and the released time of a river pollution source based on downstream sensor data monitoring the pollution concentration. The problem can be formulated as a non-convex loss minimization problem in statistical learning, and our online algorithms have vectorized and adaptive step-sizes to ensure high estimation accuracy on dimensions having different magnitudes. In order to avoid gradient-based method sticking into the saddle points of non-convex loss, the “escaping from saddle points” module and multi-start version of algorithms are derived to further improve the estimation accuracy by searching for the global minimizer of the loss functions. It can be shown theoretically and experimentally $O(N)$ local regret of the algorithms, and the high probability cumulative regret bound $O(N)$ under particular error bound condition on loss functions. A real-life river pollution source identification example shows superior performance of our algorithms than the existing methods in terms of estimating accuracy. The managerial insights for decision maker to use the algorithm in reality are also provided.

Keywords: online learning; non-convex optimization; gradient descent; pollution source identification; smart city operations

1 Introduction

Rivers are one of the most important natural resources, which can be used to act as water sources for water supply, for recreation use, to provide habitat and nourishment for organisms, and to create the majestic scenery [Sanders et al., 1990]. They appear to be vulnerable to water pollution because of their openness and accessibility over the agricultural, industrial, and municipal processes [Thibault, 2009]. The release of water pollutants into rivers, such as accidental or deliberate sewage leakage from factories or treatment plants and intentional release of toxic chemicals, threatens human health, living environment, and ecological security. According to the statistics in [Ji et al., 2017], 373 water pollution accidents happened from 2011 to 2015, some of which have caused serious consequences. Besides, the number of water pollution accidents have been on a rising tendency [Shao et al., 2006]. To mitigate the negative impacts caused by the accidents, urgent needs arise in developing an efficient approach of identifying water pollution sources (i.e., released mass, location and released time of pollution accidents), which is the foundation for quick emergency response and timely post-accident remediation.

The identification of pollution sources in rivers poses a great challenge mainly for two reasons. Firstly, the migration process explains how pollutant migrates and diffuses along the river once a pollution accident

*This research was supported by the National Research Foundation (NRF), Prime Minister’s Office, Singapore under its Campus for Research Excellence and Technological Enterprise (CREATE) program, and by Shenzhen Research Institute of Big Data (SRIBD) International Postdoctoral Fellowship. The authors are grateful to Prof. William B. Haskell for valuable comments and suggestions during the preparation of this paper.

[†]Shenzhen Research Institute of Big Data (SRIBD); Institute for Data and Decision Analytics, The Chinese University of Hong Kong, Shenzhen, China; (wenjiehuang@cuhk.edu.cn)

[‡]Department of Industrial Engineering and Management, Shanghai Jiao Tong University, Shanghai, China; NUS Environmental Research Institute, National University of Singapore, Singapore;

[§]Department of Industrial Engineering and Management, Shanghai Jiao Tong University, Shanghai, China; Department of Industrial Systems Engineering and Management, National University of Singapore, Singapore;

happens. Some elements such as velocity and dispersivity, which are the key factors for the migration process, are time-varying and environmental condition based parameters. The problem of the identification of pollution sources, which aims to trace the pollution source based on the observation of the concentration of pollution from downstream sensors, is thus an inverse problem of analyzing the migration process. Such problem is complex because of the non-linearity and uncertainties for the migration process [Wang et al., 2018]. Secondly, as streaming observations can be collected, “online” decisions on identifying pollution sources need be made to improve the speed of emergency response [Preis and Ostfeld, 2006].

The existing approaches for identifying pollutant sources are mainly categorized into three streams as below. Pollutant migration process has commonly integrated in these approaches. 1) *Analytic approach*, which directly solves the “inverse” problems (see [Li and Mao, 2011] and [Li et al., 2016]). They used the downstream monitoring sensor data to identify the pollution source information based on the Advection-Dispersion Equation models. Specifically, [Li and Mao, 2011] proposed the global multi-quadratic collocation method to identify multi-point sources in a groundwater system. [Li et al., 2016] analyzed the inverse model for the identification of pollutant sources in rivers by the global space-time radial basis collocation method. This collocation method directly induces the problem to a single-step solution of a system of linear algebraic equations in the entire space-time domain. 2) *Optimization approach*, of which the objective mainly aims to minimize the difference between the actual observation values and the theoretical values of the pollutant concentration. The implemented algorithms for analyzing the optimization model are genetic algorithm [Zhang and Xin, 2017], artificial neural network [Srivastava and Singh, 2014], simulated anneal algorithm [Jha and Datta, 2012], and differential evolution algorithm [Wang et al., 2018]. Both the analytic and optimization approaches are sensitive to uncertainties and observation noise. 3) *Statistical approach*, such as backward probability method [Wang et al., 2018], and Bayesian and Markov Chain Monte Carlo method [Hazard et al., 2014, Yang et al., 2016]. [Wang et al., 2018] obtained the source location probability based on the use of equations governing the pollutant migration process and integrated linear regression model for the source identification. [Yang et al., 2016] converts the problem by computing the posterior probability distribution of source information. Statistical approach has an advantage in dealing with noisy and incomplete prior information (Hazard et al., 2014).

These approaches for identifying pollution sources fall into “offline” fashion, which means that the identification has to be made only after all the monitoring data from sensors are collected. While in this paper, a different approach: “online” learning algorithm, is developed and analyzed to conduct a real-time estimation of pollution source information, based on streaming sensor data.

In a world where automatic data collection becomes ubiquitous, statisticians must update their paradigms to cope with new problems. Whether discussing the internet network, consumer data sets, or financial market, a common feature emerges: huge amounts of dynamic data that need to be understood and quickly processed. In real-life application, there exists *exploration-exploitation* tradeoff in decision making. For *exploitation*: the monitoring data is not adequate for accurate estimation at the early implementation stage of the sensors (i.e., cold-start problem for recommender systems), and for *exploration*: prompt and real-time action should be made for resolving the economic loss from the pollution as much as possible, once the information of the pollution source has been estimated. New approach is required to be developed to do “learning” and “optimization” simultaneously to balance such tradeoff that real-time pollution sources identification can be conducted with streaming data, and the identification result will converge to the true information as the data size grows to infinity. The algorithm will thus have plausible asymptotic performance. The data storage is another reason to limit currently approaches for real-life applications. The hardware may not be able to store the huge monitoring data produced from the sensors, and the data will become uninformative after the identification has been made. In terms of optimization point of view, most of the Advection-Dispersion Equation models (see [Van Genuchten, 1982, De Smedt et al., 2005, Wang et al., 2018]) involves complex mathematical structures (e.g. non-convex or non-smooth), such that even implementation of heuristic algorithms can attain an optimum, and it is difficult to derive the theoretical guarantee of the performance of the algorithm. Explicitly, it would be difficult to figure out the size of the streaming monitoring data such that the identification error (the gap between the estimated information and the true information of the pollution source) will be reduced to a certain precision. In this paper, our online pollution source identification technique is based on online learning and significantly different from the current studies. In next paragraph, a review on online learning (a.k.a online optimization) approaches will be given, based on which will our algorithm be developed.

Online learning technique is developed which consists of a sequence of alternating phases of observation and optimization, where data is used dynamically to make decisions in real-time. In [Shalev-Shwartz, 2012] and [Hazan, 2016], the models and algorithms for online optimization are proposed including: Online convex optimization (OCO), Online classification, Online stochastic optimization and Limit feedback (Bandit) problem. The goal of OCO algorithm is normally to minimize the *stationary regret* defined by following procedures. At each period $t \in \{1, 2, \dots, T\}$, an online decision maker chooses a feasible strategy x_t from a decision set $\mathcal{X} \subset \mathbb{R}^d$ and suffers a loss given by $f_t(x_t)$, where $f_t(\cdot)$ is a convex loss function. One key feature of online optimization is that the decision maker must make a decision for period t without knowing the loss function $f_t(\cdot)$. The stationary regret compares the accumulated loss suffered by the player with the loss suffered by the best fixed strategy. Specifically, the stationary regret for algorithm \mathcal{A} is defined as $\text{Regret}_T^{\mathcal{A}}(\{x_t\}_1^T) = \sum_{t=1}^T f_t(x_t) - \min_{x \in \mathcal{X}} \sum_{t=1}^T f_t(x)$. In [Hazan, 2016], it is shown the lower and upper regret bounds of OCO to be $\Omega(\sqrt{T})$ and $O(\sqrt{T})$ respectively. If the loss functions are strongly convex, logarithmic bounds on the regret i.e. $O(\log T)$ can be established. As suggested by its name, the loss functions in the OCO are assumed to be “convex”. Only a handful papers studied online learning with non-convex loss functions. In [Gao et al., 2018], a non-stationary regret has been proposed as performance metric, and they propose a gradient based algorithm for online non-convex learning and also derive the complexity bound $O(\sqrt{T})$ under pseudo-convexity condition. In [Hazan et al., 2017], a local regret measure is proposed, and the regret bound of gradient based algorithm is derived under mild conditions on loss functions. In [Maillard and Munos, 2010], people consider the problem of online learning in an adversarial environment when the reward functions chosen by the adversary are assumed to be Lipschitz. The cumulative regret is upper bounded by $O(\sqrt{T})$ under special geometric considerations. In [Suggala and Netrapalli, 2019] and [Agarwal et al., 2019], Follow-the-Leader algorithms are proposed that can convert online learning into offline optimization oracle. By slightly strengthening the oracle model, the online learning and offline models become computationally equivalent. In [Zhang et al., 2015], the bandit algorithm for non-convex learning is developed where the loss function specifically works on the domain of the products of decision maker’s action and adversary’s action.

Other than standard gradient based methods, in [Yang et al., 2017, Yang et al., 2018], online exponential weighting algorithms are developed for online non-convex learning problem even the decision set is non-convex. The regret bound $O(\sqrt{T \log(T)})$ is the best of our knowledge in the literature. In [Ge et al., 2015], [Jin et al., 2017], and [Levy, 2016], the authors mention the problem that even for offline non-convex optimization problem, the stationary points of non-convex objective may be local minimum, local maximum as well as saddle point, and they design algorithms that enable escaping from saddle point and reach the local minimum with a high probability. The main idea is to use random perturbed gradient and check the second-order (eigenvalue of Hessian matrix) condition.

In this paper, an online learning approach specifically for real-time river pollution source identification is developed and analyzed. Three main contributions have been made:

1. The properties a specific of Advection-Dispersion Equation (ADE) model studied in [Wang et al., 2018] is analyzed. ADE model basically simulates the dispersion of pollution in river given its parameters. Our loss function satisfies certain properties to quantify the estimation error between monitoring data and output of ADE model, analogous to the objective of statistical learning. It can be found that the loss has Lipschitz continuity as well as for its first and second derivatives. This observation inspires us to develop a gradient based online algorithm to conduct pollution source identification. Contrary to [Hazan et al., 2017], a new online non-convex learning algorithm is developed with modified step-sizes. The step-sizes are set to be vectors, meaning that the step-sizes on different dimensions (released mass, location and released time) update are different. This setting avoids the algorithm’s slow update on some dimensions while divergence on others, which improves the robustness of normal gradient descent type algorithms on the pollution source identification problems. Moreover, our algorithm is equipped with backtracking line search type technique to improve the convergence performance of the algorithm to the stationary points. Our algorithm also enables to escape from saddle points and to find a local minimum with a high probability, which will improve the quality of its real-time pollution source estimation. As a remark, it can be found that the theoretical guarantee of the algorithms is independent of the line search method applied to adjust the step-sizes, thus an analytic framework for gradient based online non-convex optimization algorithms with adjustable step-sizes is developed.
2. The performance analysis of our online learning algorithms is accomplished by deriving the explicit

$O(N/w^2 + N/w + N)$ “local” regret bound, the projected gradient of the accumulated loss (N is the size of the monitoring data and w is the window size) and also deriving the total number of gradient estimation required as $O(N/w)$ when the algorithm terminates. Then it can be shown that the optimal window size such that the local regret bound can be minimized, under fixed computational resources i.e. fixed number of gradient estimations. And the optimal window size (i.e. the size of historical data storage) is dependent on the specific properties of pollution source (choice of ADE model) and the parameters of the river (choice of the ADE model parameters), as well as the accuracy tolerance of the algorithm. For the extended algorithm with “escaping from saddle points” module, its local regret bound has the same complexity of the basic algorithm. The total number of gradient estimation of the extended algorithm to find a local minimum with a high probability is also shown. When the losses follow a specific error bound condition, the local regret bound can be linked with cumulative regret (a.k.a stationary regret), which has been widely used as a metric for online convex optimization with global optimum guarantee when the loss function and ADE model are specifically selected.

3. Our algorithms are implemented to Rhodamine WT dye concentration data from travel time study on the Truckee River between Glenshire Drive near Truckee, Calif. and Mogul, Nev. [Crompton, 2008]. The experiment results validate all our theoretical regret bounds and show that our algorithms are more superior than the existing online algorithms on all dimensions (e.g., released mass, location and released time). In addition, the multi-start version of our algorithms are developed and analyzed. It shows that the multi-start module and “escaping from saddle point” module can achieve a significantly low estimation error on certain dimensions. Thus, there are variants of online algorithms for decision makers to choose and implement, based on their own estimation accuracy requirement.

The organization of the paper is described as follows. Section 2 introduces the key notations throughout the paper and problem settings for pollution source identification. The problem is formulated, and its properties are derived. Section 3 contains the development of our online learning algorithm, the performance metrics (i.e., local and cumulative regret) of the algorithm, and the performance analysis. Section 4 serves as a remark on the issue of “escaping from saddle points” module, where includes a modified algorithm that enables finding the local minimum with a high probability. The local and cumulative regret of the algorithm are linked under an error bound condition. In Section 5, our algorithms are applied to a real-life river pollution source identification example, experimentally testing the regret bounds and comparing the performance of variants of online algorithms and existing methods in literature. The paper concludes in Section 6 with future research directions pointed out.

2 Preliminaries

In this section, the key notations throughout the paper and problem settings for pollution source identification are developed, along with the dispersion properties/model of the pollution sources.

2.1 Notations

For vectors, $\|\cdot\|$ denotes l_2 -norm, $\|\cdot\|_\infty$ denotes infinity norm and $\|\cdot\|_{\min}$ outputs the minimum element of the vector. The symbol \otimes denotes the Hadamard product of vectors and \oslash denotes the element-wise division of between two vectors. For matrices, $\lambda_{\min}(\cdot)$ denotes the smallest eigenvalues. For a function $f : \mathbb{R}^d \rightarrow \mathbb{R}$, $\nabla_x f(\cdot)$ and $\nabla_x^2 f(\cdot)$ denote the gradient and Hessian with respect to x , use $\partial f(\cdot)/\partial x$ to denote the partial derivative on x . Use $\lceil \cdot \rceil$ to denote rounding up the value to an integer. Use computational complexity notation $O(\cdot)$ to hide only absolute constants which do not depend on any problem parameter. Let $\mathbb{B}_0(r)$ denote the d -dimensional ball centered at the origin with radius r . Use $\Pi_{\mathcal{F}}$ to denote the projection onto the set \mathcal{F} defined in a Euclidean distance sense.

2.2 Problem Settings

Figure 1 shows the geometric illustration of our problem. There are facilities including factories and hospitals (marked by blue triangles) located alongside the river. Those facilities are the potential sources to discharge

pollutants. The set of sensors (denoted by M) placed in downstream cross-sections are designed to monitor the *concentration* of pollutant source, which is expressed in terms of mass per unit volume. A “sampling” is defined to be a collection of pollutant concentration detected by all sensors $m \in M$ at one time. Let $N := \{1, 2, \dots\}$ denote the set of the sort number of samplings. For each sensor, the set of the sort number of samplings is denoted N_m , having $N = \cup_{m \in M} N_m$. For n th sampling, and $n \in N$, the concentration detected by sensor m is denoted by c_m^n , and the time for the concentration data collected by sensor m is denoted by t_m^n . Let $l_m, m \in M$ denote the location of the sensor m and $L := \{l_m\}_{m \in M}$ represent the set of the location of all the sensors. Let $C^n := \{c_m^n\}_{m \in M}$ denote the set of concentration collected by all sensors for n th sampling. Once a water pollution accident happens, sensors $m \in M$ can detect a series of pollutant concentration C^n over the dynamic sampling process. Throughout the paper, assume that there is only one pollution source and released once.

The objective of this research is to develop online learning algorithm, using the collected data $\{c_m^n\}_{m \in M}$ for each sampling $n \in N$, to estimate the information of the true pollution source in real-time, including the source location l , the released time t , and the released mass s . Let (s_n, l_n, t_n) denote the estimated pollution source information at period n and (s^*, l^*, t^*) denote the true pollution source information.

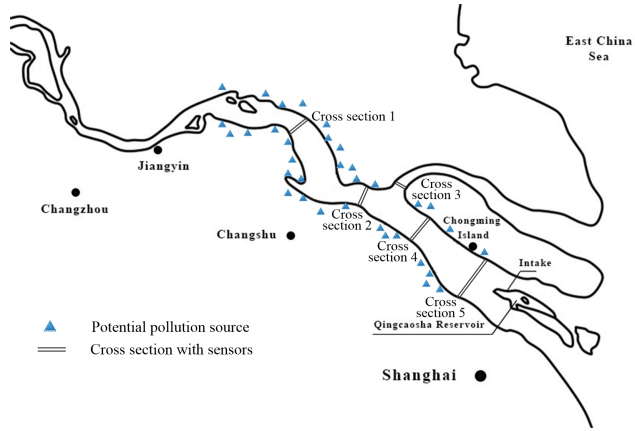


Figure 1: The river layout

2.3 Advection-Dispersion Equation (ADE)

The water pollutants are assumed to be released instantaneously from pollution sources. Once pollutants with the initial concentration s are discharged in location l and at time t , pollutants migrate and diffuse along the direction of water flow, and the pollutant concentration varies at different downstream cross-sections considering the hydrodynamic characteristics. Advection-Dispersion Equation (ADE) (see [Wang et al., 2018]) is commonly used to explain how the pollutants migrate and diffuse in the river. The analytical expression of ADE is defined as

$$C(s, l, t | l_m, t_m^n) := \frac{s}{A\sqrt{4\pi D(t_m^n - t)}} \exp \left[-\frac{(l_m - l - v(t_m^n - t))^2}{4D(t_m^n - t)} \right] \exp(-k(t_m^n - t)), \quad (2.1)$$

where A is the water area perpendicular to the river flow direction (metre²); D is the dispersion coefficient in the flow direction, which is generally evaluated by empirical equations or based on experiments (metre²/second); v is the mean flow velocity of the cross-section (metre/second); and k is the decay coefficient (second⁻¹). The physical meaning of Eq. (2.1) is explained as follows: Given the known pollution source information (s, l, t) , the theoretical estimation of the concentration level monitored by sensor m (at location l_m) at time t_m^n equals $C(s, l, t | l_m, t_m^n)$.

2.4 Problem Formulation

As briefly described in Section 2.2, the goal of the proposed method in this paper is to estimate the source information (s, l, t) , given the streaming concentration data collected by each sensor c_m^n . The following Eq.

(2.2) is then used to measure the gap between the theoretical estimation $C(s, l, t|l_m, t_m^n)$ value and the real data c_m^n :

$$\begin{aligned}\tilde{C}(s, l, t|l_m, t_m^n, c_m^n) := & \frac{s}{A\sqrt{4\pi D(t_m^n - t)}} \exp\left[-\frac{(l_m - l - v(t_m^n - t))^2}{4D(t_m^n - t)}\right] \\ & \times \exp(-k(t_m^n - t)) - c_m^n,\end{aligned}\quad (2.2)$$

For simplicity, use $\tilde{C}_{n,m}(s, l, t)$ to represent $\tilde{C}(s, l, t|l_m, t_m^n, c_m^n)$ as defined by Eq. (2.2) in the following contents of the paper. Instead of providing theoretical estimation of the downstream concentration level, given the known information (s, l, t) , the ADE model is applied in reverse engineering way: using $\tilde{C}_{n,m}(s, l, t)$ to indicate the estimation error of an estimated information (s, l, t) . Given any pollution source information estimation (s, l, t) , suppose $\tilde{C}_{n,m}(s, l, t) > 0$, then the estimated concentration monitored by sensor m at period n is *overestimated* and $\tilde{C}_{n,m}(s, l, t) < 0$ means the estimated concentration is *underestimated*.

The definition of *risk function* is given as follows which is a function on the gap $\tilde{C}_{n,m}(s, l, t)$.

Definition 2.1. Given a compact set $\mathcal{D} \subset \mathbb{R}$. Let $f : \mathcal{D} \rightarrow \mathbb{R}$ denote a risk function which satisfies:

- (i) f is Lipschitz continuous;
- (ii) f is twice differentiable;
- (iii) the first and second derivative of f are Lipschitz continuous.

There exist widely investigated loss functions in statistical learning literature satisfying conditions in Definition 2.1. The examples are shown as follows:

Example 2.2. (i) Least square (see [Agarwal and Niyogi, 2009, Wu et al., 2006]): $f(x) := x^2$ for all $x \in \mathcal{D}$.
(ii) Logistic (see [Burges et al., 2005]): $f(x) := \log[1 + \exp(x)]$ for all $x \in \mathcal{D}$.
(iii) Exponential (see [Freund et al., 2003]): $f(x) := \exp(x)$ for all $x \in \mathcal{D}$.

Given estimated information (s, l, t) , the risk function f quantifies the estimation error of sensor m at period n as $f(\tilde{C}_{n,m}(s, l, t))$. As there may exist multiple sensors downstream in the river, the aggregated estimation error of the n th period over all the sensors is defined as

$$\Psi(s, l, t|L, T^n, C^n) = \sum_{m \in M} f(\tilde{C}(s, l, t|l_m, t_m^n, c_m^n)), \quad (2.3)$$

where $T^n = \{t_m^n\}_{m \in M}$ and $C^n = \{c_m^n\}_{m \in M}$. Use $\Psi_n(s, l, t)$ to represent $\Psi(s, l, t|L, T^n, C^n)$ for simplicity. The function $\Psi_n(s, l, t)$ on (s, l, t) is called *loss function*. Use \mathcal{S} , \mathcal{L} and \mathcal{T} to denote the closed feasible set of (s, l, t) and $\mathcal{F} := \mathcal{S} \times \mathcal{L} \times \mathcal{T}$. In statistical learning, when the data C^n for all $n \in N$ are known in advance, the optimal source information (s^*, l^*, t^*) can be identified by minimizing the average loss function $\sum_{n \in N} \Psi_n(s, l, t)$. While, in online learning cases, the data C^n as well as the corresponding loss function $\Psi_n(s, l, t)$ are not completely known in advance but sequentially accessible to the decision maker. Thus, *regret* minimization method will be served as a new performance evaluation criterion other than the average loss minimizing, such that the estimation error of (s, l, t) can be measured dynamically once the a new sampling of concentration data is incorporated. The explicit definition of regret will be given latter.

2.5 Properties of Loss Functions

In this section, the mathematical properties of functions $\tilde{C}_{n,m}$ and Ψ_n will be figured out, which underlines the development of the online algorithms. Through out this paper, denote the decision variables $x = (s, l, t)$ and $x' = (s', l', t')$ for simplicity. The following assumptions on the set \mathcal{F} are first given.

Assumption 2.3. (i) \mathcal{F} is a convex and compact set. (ii) For any $t \in \mathcal{T}$, $\min_{n \in N, m \in M} \{t_m^n\} > t$ holds.
(iii) There exists $B > 0$, such that $|\Psi_n(x)| \leq B$, for any $x \in \mathcal{F}$;

Assumption 2.3 (ii) indicates that any sensor monitors data is collected after the pollution is discharged. Assumption 2.3 claims that $\tilde{C}_{n,m}$ is continuous and twice differentiable on \mathcal{F} by the following proposition.

Proposition 2.4. (i) $\tilde{C}_{n,m}$ is bounded and lipschitz continuous on the set \mathcal{F} : Given any $x, x' \in \mathcal{F}$, there exists $\sigma > 0$ such that

$$|\tilde{C}_{n,m}(x) - \tilde{C}_{n,m}(x')| \leq \sigma \|x - x'\|.$$

(ii) The first derivative of $\tilde{C}_{n,m}(x)$ is bounded and lipschitz continuous on the set \mathcal{F} : Given any $x, x' \in \mathcal{F}$, there exists $\gamma > 0$ such that

$$\|\nabla_x \tilde{C}_{n,m}(x) - \nabla_x \tilde{C}_{n,m}(x')\| \leq \gamma \|x - x'\|.$$

For Proposition 2.4 (i), it is known from Appendix: Proposition B.1, that the first derivative of $\tilde{C}_{n,m}(x)$ on \mathcal{F} is bounded. From [Sohrab, 2014], it can be shown that $\tilde{C}_{n,m}(x)$ is Lipschitz continuous on \mathcal{F} with a certain modulus $\sigma > 0$. Since $\tilde{C}_{n,m}(x)$ is twice differentiable on \mathcal{F} , then the boundedness of second derivatives in Appendix: Proposition B.1 can be proved, which leads to the Lipschitz continuity of $\tilde{C}'_{n,m}$ on \mathcal{F} . The following proposition shows the Lipschitz continuity of function Ψ_n as well as its first and second derivatives on \mathcal{F} , with the proof attached in the Appendix.

Proposition 2.5. (i) Ψ_n is lipschitz continuous on \mathcal{F} : Given any $x, x' \in \mathcal{F}$, there exists $\kappa > 0$ such that

$$\|\Psi_n(x) - \Psi_n(x')\| \leq \kappa \|x - x'\|.$$

(ii) Ψ_n is β -smooth on \mathcal{F} : Given any $x, x' \in \mathcal{F}$, there exists $\beta > 0$ such that

$$\|\nabla_x \Psi_n(x) - \nabla_x \Psi_n(x')\| \leq \beta \|x - x'\|.$$

(iii) Ψ_n is also ι -Hessian Lipschitz: Given any $x, x' \in \mathcal{F}$, there exists $\iota > 0$ such that

$$\|\nabla_{(s, l, t)}^2 \Psi_n(x) - \nabla_{(s, l, t)}^2 \Psi_n(x')\| \leq \iota \|x - x'\|.$$

As a remark, the function Ψ_n constructed from ADE model (2.1) and any loss function satisfying conditions in Definition 2.1 is just a specific case of any function Ψ_n satisfying the conditions in Proposition 2.5. As a remark, any function Ψ_n satisfying the conditions in Proposition 2.5 is applicable by our approach.

Next, the definition of “projected gradient” is provided and its properties are derived. Those properties will be useful in designing and analyzing our online algorithms. Those properties are naturally extended from [Hazan et al., 2017] where the step-size η is univariate rather a vector in our case.

Definition 2.6. (Projected gradient) Let $\Psi_n : \mathcal{F} \rightarrow \mathbb{R}$ be a differentiable function on compact and convex set \mathcal{F} . Let vector-valued step size be $\eta \in \mathbb{R}_+^d$ (throughout the paper, $d = 3$ for pollution source identification problems), and define $\nabla_{\mathcal{F}, \eta} \Psi_n : \mathcal{F} \rightarrow \mathbb{R}^d$, the (\mathcal{F}, η) -projected gradient of Ψ_n , by

$$\nabla_{\mathcal{F}, \eta} \Psi_n(x) := (x - \Pi_{\mathcal{F}}[x - \eta \otimes \nabla_x \Psi_n(x)]) \oslash \eta,$$

where $\Pi_{\mathcal{F}}[\cdot]$ denotes the orthogonal projection onto \mathcal{F} , and the symbol \otimes denotes the Hadamard product and \oslash denotes the element-wise division of two vectors.

Proposition 2.7. Let \mathcal{F} be a compact and convex set and suppose $\Psi_n : \mathcal{F} \rightarrow \mathbb{R}$ satisfies the properties in Proposition 2.5. Then, there exists some point $x^* \in \mathcal{F}$ for which

$$\nabla_{\mathcal{F}, \eta} \Psi_n(x^*) = 0.$$

The proof of Proposition 2.7 follows from [Hazan et al., 2017, Proposition 2.3]. Since $\nabla_x \Psi_n(x)$ is continuous function on \mathcal{F} , then the composition function $g(x) := \Pi_{\mathcal{F}}[x - \eta \otimes \nabla_x \Psi_n(x)]$ is therefore continuous. Thus g satisfies the conditions for Brouwer’s fixed point theorem, implying that there exists some $x^* \in \mathcal{F}$ for which $g(x^*) = x^*$. At this point, the projected gradient vanishes. The final proposition noted here is that an approximate local minimum, as measured by a small projected gradient, is robust with respect to small perturbations, with the proof attached in the Appendix.

Proposition 2.8. Let x be any point in \mathcal{F} , and let Ψ and Φ be differentiable functions $\mathcal{F} \rightarrow \mathbb{R}$. Then for any $\eta \in \mathbb{R}_+^d$ and $x \in \mathcal{F}$,

$$\|\nabla_{\mathcal{F}, \eta}[\Psi + \Phi](x)\| \leq \|\nabla_{\mathcal{F}, \eta} \Psi(x)\| + \|\nabla \Phi(x)\|.$$

Algorithm 1 Adaptive time-smoothed online gradient descent (ATGD)

Input: window size $w \geq 1$, tolerance $\delta > 0$, constant $K > 0$, and a convex set \mathcal{F} ;
Set $x_1 \in \mathcal{F}$ arbitrarily
for $n = 1, \dots, N$ **do**
 Observe the cost function $\Psi_n : \mathcal{F} \rightarrow \mathbb{R}$.
 Compute the initial step-size: $\eta_0 = \mathfrak{S}(F_{n,w}, K)$.
 Initialize $x_{n+1} := x_n$ and $\eta_n := \eta_0$.
 while $\|\nabla_{\mathcal{F}, \eta_n} F_{n,w}(x_{n+1})\|_2 > \delta$ **do**
 Determine η_n using Normalized Backtracking-Armijo line search (Algorithm 2).
 Update $x_{n+1} := x_{n+1} - \eta_n \otimes \nabla_{\mathcal{F}, \eta_n} F_{n,w}(x_{n+1})$.
 end while
end for

3 The Algorithm

In this section, our basic algorithm (Algorithm 1): Adaptive time-smoothed online gradient descent (ATGD), is developed. The key idea of this algorithm is to play follow-the-leader iterates, approximated to a suitable tolerance using projected gradient descent. Apart from the standard gradient descent paradigm, the improvements our algorithm are: (i) adjusting the step-sizes to be vectors, meaning that the algorithm performs different step-sizes on different dimensions (released mass, location and released time). This setting avoids potentially slow update on some dimensions and divergence on other dimensions, due to the different magnitude of gradient on different dimensions (i.e., steep surface will have high gradient magnitude and flat surface will have low gradient magnitude). The vectorized step-sizes setting thus improves the robustness of the algorithm than the univariant step-size version; (ii) in practice, the convergence of the algorithms to a saddle point (first-order stationary point but not a local minimum) will be slow or even not guaranteed if the step-size has not been tuned well. To tackle this problem, the algorithm is equipped with adaptive step-sizes modified from Backtracking-Armijo line search, which is one of the most widely investigated inexact line search method (see [Dennis Jr and Schnabel, 1996, Armijo, 1966, Nocedal and Wright, 2006]).

In Algorithm 1 & 2, function $F_{n,w}$ is sliding-window time average of losses (where w denotes the window size) and $\mathfrak{S}(F_{n,w}, K)$ is an operator choosing the initial step-sizes whose explicit definition will be given latter. As shown in Algorithm 1, the iteration t tracks the gradient descent update in the “while” loop. The explicit description of normalized Backtracking-Armijo line search is shown in Algorithm 2, where a properly chosen β prevents the step-size from getting too large along the gradient descent direction, and the backtracking method prevents the step-size from getting too small. Here the Armijo condition is imposed on normalized gradient to further reduce the negative effect of gradient magnitude difference on each dimension, in addition to the vector step-sizes setting. Term $\eta^{(l)} \beta \|\nabla_{\mathcal{F}, \eta^{(l)}} F_{n,w}(x_{n+1})\|_2$ at the right side of the Armijo inequality will approach zero when the norm of projected gradient approaches zero, and then the condition will become standard Backtracking line search. This setting leads to faster convergence near the stationary points. Algorithm 2 will always terminate since its stopping criterion is relaxed from standard Backtracking-Armijo line search. Explicitly, the termination can also be proved by limit of Taylor series. Given the Taylor expansions for the two terms:

$$\begin{aligned} & F_{n,w}(x_{n+1} - \eta^{(l)} \otimes \nabla_{\mathcal{F}, \eta^{(l)}} F_{n,w}(x_{n+1}) / \|\nabla_{\mathcal{F}, \eta^{(l)}} F_{n,w}(x_{n+1})\|_2) \\ & \leq F_{n,w}(x_{n+1}) - \|\eta^{(l)}\|_{\min} \|\nabla_{\mathcal{F}, \eta^{(l)}} F_{n,w}(x_{n+1})\|_2 + O(\|\eta^{(l)}\|_{\infty}^2), \end{aligned}$$

and

$$F_{n,w}(x_{n+1}) + \beta \|\eta^{(l)} \otimes \nabla_{\mathcal{F}, \eta^{(l)}} F_{n,w}(x_{n+1})\|_2 \leq F_{n,w}(x_{n+1}) + \beta \|\eta^{(l)}\|_{\min} \|\nabla_{\mathcal{F}, \eta^{(l)}} F_{n,w}(x_{n+1})\|_2.$$

Obviously, by examining the limit of the two terms when each element of $\eta^{(l)}$ is approaching zero, the condition in Algorithm 2 for entering the “while” loop will be violated and thus the algorithm will terminate.

In terms of the way of choosing a proper initial step-sizes, the main idea is to set the initial step-sizes on each dimension inversely proportional to the Lipschitz modulus of the loss on that dimension, such that the algorithm can adjust the identification change on each dimension to the similar magnitude. A simple

Algorithm 2 Normalized Backtracking-Armijo line search

Input: $\eta_0 > 0$, x_{n+1} and $F_{n,w}$, let $\eta^{(0)} = \eta_0$ and $l = 0$.
while $F_{n,w}(x_{n+1} - \eta^{(l)} \otimes \nabla_{\mathcal{F}, \eta^{(l)}} F_{n,w}(x_{n+1}) / \|\nabla_{\mathcal{F}, \eta^{(l)}} F_{n,w}(x_{n+1})\|_2) > F_{n,w}(x_{n+1}) + \beta \|\eta^{(l)} \otimes \nabla_{\mathcal{F}, \eta^{(l)}} F_{n,w}(x_{n+1})\|_2$ **do**
 Set $\eta^{(l+1)} = \tau \otimes \eta^{(l)}$, where $\tau \in (0, 1)^d$ is fixed (e.g., $\tau = (1/2, 1/2, 1/2)$),
 Set $l = l + 1$
end while
Set $\eta_n = \eta^{(l)}$

partition method is first derived to derive a lower bound on the Lipschitz modulus on each dimension from [Gimbutas and Žilinskas, 2016, Sergeyev et al., 2013, Pintér, 2013]. At iteration $n \leq N$, generate K^3 points on the cube \mathcal{F} denoted as (s^1, \dots, s^K) , (l^1, \dots, l^K) and (t^1, \dots, t^K) . In each dimension, adjacent points have equal distance. Compute

$$\kappa_n^s = \max_{i,j,k,p=1,\dots,K} \left\{ \frac{|F_{n,w}(s^i, l^k, t^p) - F_{n,w}(s^j, l^k, t^p)|}{|s^i - s^j|} : i \neq j \right\},$$

$$\kappa_n^l = \max_{i,j,k,p=1,\dots,K} \left\{ \frac{|F_{n,w}(s^k, l^i, t^p) - F_{n,w}(s^k, l^j, t^p)|}{|l^i - l^j|} : i \neq j \right\},$$

and

$$\kappa_n^t = \max_{i,j,k,p=1,\dots,K} \left\{ \frac{|F_{n,w}(s^k, l^p, t^i) - F_{n,w}(s^k, l^p, t^j)|}{|t^i - t^j|} : i \neq j \right\},$$

to be the Lipschitz modulus estimation on dimension s , l and t respectively. Let $\eta_0 \in \mathbb{R}_+^d$ denote initial step-sizes at iteration n with the step-sizes on each dimension as η_0^s , η_0^l and η_0^t . Then η_0 should satisfies the following two condition: (i) for the validation and analysis of the algorithm, choose sufficiently large initial step-size such that $\|\eta_0\|_{\min} / \|\eta_0\|_\infty^2 \gg \beta/2$; and (ii) the equations

$$\frac{\eta_0^s}{\kappa_n^s} = \frac{\eta_0^l}{\kappa_n^l} = \frac{\eta_0^t}{\kappa_n^t},$$

hold. For simplicity, use the operator \mathfrak{S} to encode the process of finding an initial step-size. Given the function $F_{n,w}$ and constant $K > 0$, the initial step-size is $\eta_0 = \mathfrak{S}(F_{n,w}, K)$.

In the following subsection, two kinds of “regret” definition are presented which measure the performance of online learning algorithm.

3.1 Local and Cumulative Regret

As mentioned at the end of Section 2.4, when implementing Algorithm 1, the data C^n as well as the corresponding loss function $\Psi_n(s, l, t)$ are unknown in advance but sequentially accessible to the decision maker. *Regret* minimization method will be served as a new performance evaluation criterion other than the average loss minimizing, such that the estimation error of (s, l, t) can be measured dynamically once the a new sampling of concentration data is incorporated.

In the well-established framework of online convex optimization, numerous algorithms can efficiently achieve optimal regret, in the sense of converging in terms of total accumulated loss towards the best fixed decision in hindsight (see [Hazan, 2016] and [Shalev-Shwartz, 2012]). The “cumulative regret” is defined as follows.

Definition 3.1. (Cumulative regret) Given an online learning algorithm \mathcal{A} , its cumulative regret (a.k.a stationary regret) after N iterations is denoted by

$$\mathfrak{R}^{\mathcal{A}}(N) := \sum_{n=1}^N \Psi_n(x_n) - \inf_{x \in \mathcal{F}} \sum_{n=1}^N \Psi_n(x). \quad (3.1)$$

If the cumulative regret of \mathcal{A} is bounded by $O(N)$, which also means that the average cumulative regret of \mathcal{A} is bounded, then \mathcal{A} is acceptable. That is, for any $x \in \mathcal{F}$, one can play iterates x_1, \dots, x_N such that

$$\frac{1}{N} \sum_{n=1}^N [\Psi_n(x_n) - \Psi_n(x)] = O(1).$$

Unfortunately, even in the offline non-convex optimization case, it is too ambitious to converge towards a global minimizer in hindsight. The global convergence of offline non-convex optimization is normally NP-hard. In the existing literature, it is usual to state convergence guarantees towards an ϵ -approximate stationary point that is, there exists some iterate x_n for which $\|\nabla \Psi_n(s_n, l_n, t_n)\|^2 \leq \epsilon$. In light of the computational intractability of direct analogues of convex regret, the definition of “local regret” is given, a new notion of regret which quantifies the objective of predicting points with small gradients on average.

Throughout this paper, for convenience, the following notation follows from [Hazan et al., 2017] to denote the sliding-window time average of functions, parameterized by some window size $1 \leq w \leq N$:

$$F_{n,w}(x) := \frac{1}{w} \sum_{i=0}^{w-1} \Psi_{n-i}(x).$$

For simplicity, define $\Psi_n(x)$ to be identically zero for all $n \leq 0$.

Definition 3.2. (Local regret) [Hazan et al., 2017, Definition 2.5] Fix some $\eta > 0$. Define the w -local regret of an online algorithm as:

$$\mathfrak{R}_w(N) := \sum_{n=1}^N \|\nabla_{\mathcal{F}, \eta} F_{n,w}(x_n)\|^2. \quad (3.2)$$

In [Hazan et al., 2017], the necessity of time smoothing term w is argued that for any online algorithm, an adversarial sequence of loss functions can force the local regret incurred to scale with N as $O(N/w^2)$. In addition, for some online learning problem where $F_{n,w}(x) \approx \Psi_n(x)$, a bound on local regret truly captures a guarantee of playing points with small gradients. On the other hand, Algorithm 1 treats $F_{n,w}$ as the follow-the-leader objective when estimating x_{n+1} . Instead of summing up all the historical loss functions up to iteration n , the follow-the-leader objective considers recording and summing up w previous loss functions. This setting saves the storage when implementing the online algorithm as mentioned in Section 1. In addition, It will be latter shown that the performance of online non-convex learning algorithms can be measured by cumulative regret, if the local properties on the local minimizer of Ψ_n and $\sum_{n=1}^N \Psi_n$ are attained.

3.2 Performance Analysis

In this subsection, the analysis of regret bound (i.e., the upper bound on the local regret) for Algorithm 1 is shown as well as the derivation of the optimal window size selection to minimize the regret bound within limited number of gradient estimations. Our method efficiently achieves a local regret bound of $O(T/w^2)$, taking $O(Tw)$ iterations of inner loop (w here denotes the window size). It can also be shown how to select the optimal window size w^* when fixing computational resources i.e. fixing number of gradient estimations, such that the local regret bound can be minimized. The following Theorem 3.3 presents the local regret and the total number of required gradient estimation. The proof of Theorem 3.3 is given in Section C.

Theorem 3.3. *Let Ψ_1, \dots, Ψ_N be the sequence of loss functions presented to Algorithm 1, satisfying the properties in Proposition 2.5. Then:*

(i) *Then w -local regret incurred satisfies*

$$\mathfrak{R}_w(N) \leq (\delta + \frac{2\kappa}{w})^2 N. \quad (3.3)$$

(ii) *There exists $\eta' \leq \eta_0$, such that the total number of gradient steps taken by Algorithm 1 is bounded by:*

$$\frac{2B}{\delta^2 \left(\|\eta'\|_{\min} - \frac{\beta \|\eta_0\|_{\infty}^2}{2} \right) w} N. \quad (3.4)$$

Theorem 3.3 illustrates that Algorithm 1 attains local regret bound $O(N/w^2 + N/w + N)$ with $O(N/w)$ gradient evaluation steps. Theorem 3.3 (i) illustrates that ATGD is acceptable with average cumulative regret $O(1)$. Besides, the bound (3.4) is higher than the bound in [Hazan et al., 2017, Algorithm 1] due to the diminishing step-sizes, which will lead to more gradient estimations of Algorithm 1 than [Hazan et al., 2017, Algorithm 1], while lead to lower local regret bound than [Hazan et al., 2017, Algorithm 1] given the fixed number of gradient estimations. The results reveal a tradeoff between low computational complexity and high convergence guarantee. Moreover, our results show that for a fixed streaming data size N , increasing the window size w i.e. increasing the smoothing effect will reduce both the complexity of local regret and total number of gradient steps.

In terms of the lower bound on local regret, it is shown from [Hazan et al., 2017, Theorem 2.7] that for any online algorithm, an adversarial sequence of loss functions can force the local regret incurred to scale with N as $\Omega(N/w^2)$.

The next question is: How to select the optimal window size w^* when fixing computational resources i.e. fixing number of gradient estimations, such that the local regret bound can be minimized? By fixing the bound on the total number of gradient steps as T , then the required size of input data would be

$$N = \frac{\delta^2 \left(\|\eta'\|_{\min} - \frac{\beta \|\eta_0\|_\infty^2}{2} \right) w}{2B} T.$$

The bound on the w -local regret would become

$$\left[\delta^2 w + 4\delta\kappa + \frac{4\kappa^2}{w} \right] \frac{\delta^2 \left(\|\eta'\|_{\min} - \frac{\beta \|\eta_0\|_\infty^2}{2} \right)}{2B} T.$$

By minimizing the w -local regret in w , the optimal window size w^* equals 1 if $2\kappa/\delta \leq 1$, and equals N if $2\kappa/\delta \geq N$. When $1 < 2\kappa/\delta < N$, the optimal window size w^* equals $2\kappa/\delta$. Thus the optimal window size w^* is dependent on the Lipschitz continuous modulus of function Ψ_n as well as the tolerance level δ , but is independent on the gradient step-sizes as well as the computational budget. To interpret, the more “fluctuation” the shape of loss functions have and the more accurate estimation requirement on the algorithm is, the larger the required window sizes should be chosen. In another word, the optimal window size (i.e. the size of historical data storage) should be determined based on the specific properties of pollution source (choice of ADE model) and the parameters of the river (choice of the ADE model parameters).

Remark 3.4. (i) Suppose the step-sizes are stationary of Algorithm 1, where step-sizes $\{\eta_t\}$ are replaced with η_0 and Backtracking-Armijo line search step will not be implemented. Then Theorem 3.3 will still hold for the new algorithm by replacing η' with η_0 in the bound (3.4). When $\{\eta_t\}$ become stationary and uni-varient value, Algorithm 1 becomes [Hazan et al., 2017, Algorithm 1]. Thus our Algorithm 1 generalizes [Hazan et al., 2017, Algorithm 1].

(ii) From the proof of Theorem 3.3 in the Appendix, the theoretical guarantee of Algorithm 1 summarized in the theorem is independent of the structure of inner loop updating the step-sizes. In other words, Algorithm 2 can be replaced with other adaptive step-size approach other than Backtracking-Armijo line search (e.g. Generic line search, Exact line search) only if those methods continue to reduce the step-sizes when the stopping criterion is not satisfied. Thus, an analytic framework for gradient based online non-convex optimization algorithms is developed with adjusted step-sizes by line search.

4 Escaping from Saddle Points

In this section, the basic algorithm (Algorithm 1) is further extended in terms of its practical implementation, by deriving the module “escaping from saddle points” which helps the algorithm arriving at a local minima with a high probability instead of being stuck into any first-order stationary point. It can also be shown the cumulative regret of the algorithm under an error bound condition on the loss functions.

In non-convex optimization, the convergence to first-order stationary points (points where first-order derivative equals zero) is not satisfactory. For non-convex functions, first-order stationary points can be global minima, local minima, saddle points or even local maxima. For many non-convex problems, it is

Algorithm 3 Adaptive perturbed time-smoothed online gradient descent (APTGD)

Input: window size $w \geq 1$, Constant $c \leq 1$, tolerance $\delta > 0$, contant $K > 0$, and a convex set \mathcal{F} ;

Input: $\chi = 3 \max \left\{ \log \left(\frac{d\kappa \Delta f}{c\delta^2 \epsilon} \right), 4 \right\}$, $r = \frac{\sqrt{c}}{\chi^2} \cdot \frac{\delta}{\kappa}$, $g_{\text{thres}} = \frac{\sqrt{c}}{\chi^2} \cdot \delta$, $f_{\text{thres}} = \frac{c}{\chi^3} \sqrt{\frac{\delta^3}{\iota}}$, $t_{\text{thres}} = \lceil \frac{\chi}{c^2} \cdot \frac{\kappa}{\sqrt{\iota} \delta} \rceil$, $t_{\text{noise}} = -t_{\text{thres}} - 1$

Set $x_1 \in \mathcal{F}$ arbitrarily.

for $n = 1, \dots, N$ **do**

- Observe the cost function $\Psi_n : \mathcal{F} \rightarrow \mathbb{R}$.
- Compute the initial step-size: $\eta_0 = \mathfrak{S}(F_{n,w}, K)$.
- Initialize $x_{n+1} := x_n$ and t_{noise} ;
- for** $t = 0, 1, \dots$ **do**

 - Initialize $x_{n+1}^t := x_{n+1}$;
 - Determine η_t using Normalized Backtracking-Armijo line search (Algorithm 2).
 - if** $\|\nabla_{\mathcal{F}, \eta_t} F_{n,w}(x_{n+1}^t)\| \leq g_{\text{thres}}$ and $t - t_{\text{noise}} > t_{\text{thres}}$ **then**

 - $t_{\text{noise}} = t$, $\tilde{x}_{n+1}^t = x_{n+1}^t$, $x_{n+1}^t = \tilde{x}_{n+1}^t + \omega$ where ω uniformly sampled from $\mathbb{B}_0(r)$
 - if** $t - t_{\text{noise}} = t_{\text{thres}}$ and $F_{n,w}(x_{n+1}^t) - F_{n,w}(\tilde{x}_{n+1}^{t_{\text{noise}}}) > -f_{\text{thres}}$ **then**

 - Return** $x_{n+1} = \tilde{x}_{n+1}^{t_{\text{noise}}}$

 - Update $x_{n+1}^{t+1} = x_{n+1}^t - \eta_t \otimes \nabla_{\mathcal{F}, \eta_t} F_{n,w}(x_{n+1}^t)$.

- end for**

end for

sufficient to find a local minimum. In each iteration n in our basic algorithm: ATGD, the algorithm will terminates when x_n is the δ -first-order stationary point of the follow-the-leader iterate $F_{n,w}$ on \mathcal{F} . However, such point may not necessarily be the local minimum of Ψ_n . Additional techniques are required that can escape all saddle points and arrive at local minima.

Following the settings in [Jin et al., 2017], given a fixed $\tilde{\epsilon} > 0$, consider finding $\tilde{\epsilon}$ -second-order stationary point for Ψ_n on \mathcal{F} . For ι -Hessian Lipschitz functions, these points are defined in [Nesterov and Polyak, 2006] as

$$\|\nabla_x \Psi_n(x)\| \leq \tilde{\epsilon}, \quad \text{and} \quad \lambda_{\min}(\nabla_x^2 \Psi_n(x)) \geq -\sqrt{\iota \tilde{\epsilon}},$$

where $\lambda_{\min}(\cdot)$ outputs the minimal eigenvalue of a matrix and ι is the Lipschitz modulus of $\nabla_x^2 \Psi_n(x)$ defined in Proposition 2.5(iii). Second-order stationary points are very important in non-convex optimization because when all saddle points are strict ($\lambda_{\min}(\nabla_x^2 \Psi_n(x)) < 0$), all second-order stationary points are exactly local minima. A robust version of “strict saddle” condition is next provided based on [Ge et al., 2015, Jin et al., 2017], which shows that function Ψ_n satisfies “strict saddle” condition.

Assumption 4.1. Function $\Psi_n(\cdot)$ is (θ, τ, ζ) -strict saddle with $\theta, \tau > 0$ and $\zeta \geq 0$. That is, for any x , at least one of the following holds: (i) $\|\nabla_x \Psi_n(x)\| \geq \theta$. (ii) $\lambda_{\min}(\nabla_x^2 \Psi_n(x)) \leq -\tau$. (iii) x is ζ -close to the set of local minima of Ψ_n .

Intuitively, the strict saddle property states that the \mathcal{F} space can be divided into three regions: 1) a region where the gradient is large; 2) a region where the Hessian has a significant negative eigenvalue (around saddle point); and 3) the region close to a local minimum. It is straightforward to verify that Assumption 4.1 holds for function Ψ_n , since condition in Assumption 4.1 (iii) holds for all $x \in \mathcal{F}$.

Algorithm 3 is a perturbed form of gradient descent algorithm. For each iteration n in Algorithm 3, the algorithm will search the solution where the current gradient is small ($\leq \delta$) (which indicates that the current iterate x_n^t is potentially near a saddle point), the algorithm adds a small random perturbation to the gradient. The perturbation is added at most only once every t_n^{thres} iterations. If the function value does not decrease enough (by f_n^{thres}) after t_n^{thres} iterations, the algorithm will outputs $x_n^{t_n^{\text{noise}}}$ which can be proved to be necessarily close to a local minima. The step-size choice operator $\mathfrak{S}(F_{n,w}, K)$, instead of requiring the condition $\|\eta_0\|_{\min}/\|\eta_0\|_{\infty}^2 \gg \beta/2$ in Algorithm 1, requires $\|\eta_0\|_{\infty} = c/\kappa$ in Algorithm 3.

Theorem 4.2. Let Ψ_n satisfies properties in Proposition 2.5 and 4.1. There exists an absolute constant $c_{\max} \leq 1$ such that, for $c \leq c_{\max}$, and $\Delta f \geq \max_{n=1, \dots, N} \{F_{n,w}(x_{n-1})\}$ by letting $\delta := \min(\theta, \tau^2/\iota)$, Algorithm 3 will output sequence of δ -second-order stationary points which are also the ζ -close local minima

of $\{F_{n,w}\}_{n=1, \dots, N}$, with probability $1 - \epsilon$, and terminate in the following total number of iterations (gradient estimations):

$$O\left(\frac{\kappa\Delta f}{\delta^2} \log^4\left(\frac{d\kappa\Delta f}{\delta^2\epsilon}\right) \bar{N}\right). \quad (4.1)$$

The proof of Theorem 4.2 is shown in Appendix which follows the results in [Jin et al., 2017]. Here their results can be naturally extended on standard gradient descent to online gradient descent since our basic algorithm contains an offline follow-the-leader oracle at each period. Theorem 4.2 shows that by careful selection of Δf and δ , the algorithm will output the local minima of each follow-the-leader oracle in each period with a sub-linear number of iterations in a high probability. As mentioned in [Jin et al., 2017], Theorem 4.2 only explicitly asserts that the output will lay within some fixed radius ζ from a local minimum. In many real applications, ζ can be further written as a function $\zeta(\cdot)$ of gradient threshold θ , so that when θ decreases, $\zeta(\theta)$ decreases linearly or polynomially depending on θ . Therefore, in these cases, Theorem 4.2 further gives a convergence rate to a local minimum.

Next, the local regret can be linked with the cumulative regret of Algorithm 3 under a specific error bound condition at any local minimum of functions $\frac{1}{n} \sum_{i=1}^n \Psi_i$ and Ψ_n for all $1 \leq n \leq N$. And the cumulative regret can be shown to be bounded by $O(N)$. In another word, the global optimum performance of Algorithm 3 can be investigated for carefully chosen loss function f and specific sensor data.

Definition 4.3. (Error bound condition) Let $x_N^* = (s_N^*, l_N^*, t_N^*)$ be any minimizer of $\frac{1}{N} \sum_{n=1}^N \Psi_n$, then the error bound condition holds with parameters (ζ, μ) if for any x in the ζ -domain of x_N^* , there exists $\mu > 0$, such that

$$\|\nabla_{\mathcal{F},\eta} F_{N,N}(x)\| \geq \mu \left[\frac{1}{N} \sum_{n=1}^N \Psi_n(x) - \frac{1}{n} \sum_{n=1}^N \Psi_n(x_N^*) \right].$$

Given any $1 \leq n \leq N$. Let $x^{n,*} = (s^{n,*}, l^{n,*}, t^{n,*})$ be by any minimizer of Ψ_n , then the (ζ, μ) error bound condition is: for any x in the ζ -domain of $x^{n,*}$ with $\zeta > 0$, there exists $\mu > 0$, such that

$$\|\nabla_{\mathcal{F},\eta} F_{n,1}(x)\| \geq \mu [\Psi_n(x) - \Psi_n(x^{n,*})],$$

for all $n \leq N$.

Definition 4.3 is an extension from [Drusvyatskiy and Lewis, 2018, Definition 3.1] that holds for sliding-window time average of functions $F_{n,1}(\cdot)$ for all $n = 1, \dots, N$ and $F_{N,N}(\cdot)$. They are called Polyak-Lojasiewicz (PL) inequality showing projected gradient grows as a quadratic function as the functions Ψ_n , $n = 1, \dots, N$ and $\frac{1}{N} \sum_{n=1}^N \Psi_n$ are increased. Next, an example of choosing f as Least square loss is shown.

Example 4.4. Suppose choose f to be Least square, if the following two conditions are satisfied for the sensor data in ADE model: (i) function $\tilde{C}_{n,m}$ is bi-Lipschitz continuous on the ζ -domain of x_N^* and $x^{n,*}$ for all $n \leq N$, such that there exists $\sigma' \leq 1$ and

$$|\tilde{C}_{n,m}(x) - \tilde{C}_{n,m}(x_N^*)| \geq \sigma' \|x - x_N^*\|,$$

for any x in the ζ -domain of x_N^* , and

$$|\tilde{C}_{n,m}(x) - \tilde{C}_{n,m}(x^{n,*})| \geq \sigma' \|x - x^{n,*}\|,$$

for any x in the ζ -domain of $x^{n,*}$; (ii) function $\tilde{C}_{n,m}$ is convex on the ζ -domain of x_N^* and $x^{n,*}$ for all $n \leq N$. Then the corresponding functions Ψ_n and $\frac{1}{n} \sum_{i=1}^n \Psi_i$ for all $1 \leq n \leq N$ satisfies the error bound condition with in Definition 4.3, and here choose $\mu = 4\sigma' |M|$.

The detailed interpretation and analysis of Example 4.4 is given in the Appendix. The following Theorem 4.5 provides a high probability bound for the cumulative regret of Algorithm 2 with $O(N)$. with the proof attached in the Appendix.

Theorem 4.5. Let Ψ_n satisfies properties in Proposition 2.5 and 4.1 and functions Ψ_n and $\frac{1}{n} \sum_{i=1}^n \Psi_i$ for all $1 \leq n \leq N$ satisfies the error bound condition with in Definition 4.3, then with probability $1 - \epsilon$, the cumulative regret of Algorithm 3 after

$$O \left(\frac{\kappa \Delta f}{\delta^2} \log^4 \left(\frac{d \kappa \Delta f}{\delta^2 \epsilon} \right) N \right).$$

gradient estimations, with $\Delta f \geq \max_{n=1, \dots, N} \{F_{n,w}(x_{n-1})\}$ and $\delta := \min(\theta, \tau^2/\iota)$, is bounded by

$$O \left(\frac{\delta + 2\kappa}{\mu} \cdot N \right). \quad (4.2)$$

Remark 4.6. For practical implementation, the multi-start version algorithms could be developed for both ATGD and APTGD. The main idea is to create several solution paths when implementing the algorithms given different start points. In each iteration, the square of the difference between ADE value and real concentration data for each sensor is recorded. Following the idea from [Jiang et al., 2015], the minimizer of the average of the square of the difference over all the sensors, among all the solution paths, is chosen, and treat it as the estimated optimal solution at that iteration. Practically, the multi-start implementation can increase the chance to find more accurate source information estimation. The explicit structures of multi-start algorithms are shown as Algorithm 4 (MTGD) and Algorithm 5 (MPTGD) in Appendix A.

5 Experiments and Application

In this section, the experiments validating the theoretical result of our online learning algorithms are conducted, and our methods are also applied to real-life river pollution source identification problems. For the experiments, use the Rhodamine WT dye concentration data from travel time study on the Truckee River between Glenshire Drive near Truckee, Calif. and Mogul, Nev. [Crompton, 2008]. Figure 2 presents locations of a pollutant site marked by a black star and four sampling sites marked by red stars. The data includes the true pollutant source information (s, l, t) and 82 pairs of concentration data detected in the downstream four sampling sites. The parameters in the ADE model are obtained from [Crompton, 2008] and [Jiang et al., 2017], namely, $v = 80 \text{ m/min}$, $D = 2430 \text{ m}^2/\text{min}$, $A = 60 \text{ m}^2$, and $k = 10^{-8} \text{ min}^{-1}$.

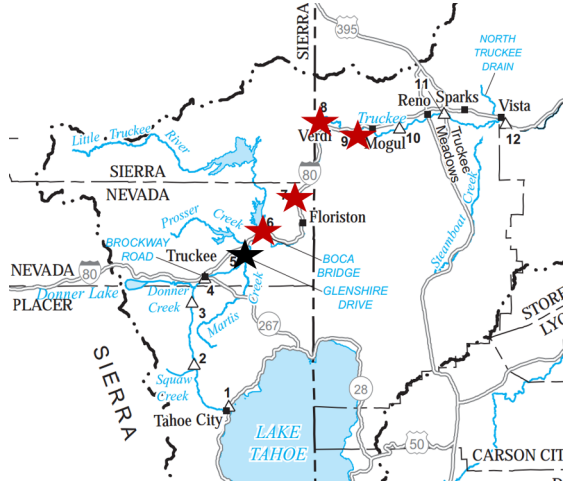


Figure 2: Locations of pollutant site and sampling sites on the Truckee River

5.1 Experiment I: Regret Analysis

In this experiment, real data is used to compute the local regret bound (3.2) and the cumulative regret bound (3.1) for various online algorithms, including: [Hazan et al., 2017, Algorithm 1], ATGD, APTGD, MTGD

and MPTGD. Choose the loss function f to be Least square (i.e., $f(x) = x^2$) and window size $w = 1$. The group size (number of multi-starts) are chosen as $I = 30$ in the multi-start algorithms. The initial step-sizes are chosen by the method summarized in Section 3.1. The experiment results are recorded from Figure 3 to Figure 7. These figures validate that all of those algorithm has local regret bound $O(N)$ as inequality (3.3), and they also show experimentally that the cumulative regret of all those algorithm has complexity $O(N)$ which potentially conforms to the bound (4.2). In addition, ATGD, APTGD, MPGD and MPTGD have superior local regrets than [Hazan et al., 2017, Algorithm 1], which reveals that the vectorized and adaptive step-sizes improve the performance on the pollution source identification problem than the fixed and univariate step-sizes algorithm. From the plots of cumulative regret of APTGD and MPTGD, it can be observed that adding the “escaping from saddle points” module can reduce the growth rate of the cumulative regrets, which means that as the size of data grows, the algorithms are outputting the solution closer to the global minimizer a.k.a., the true source information. The plots of cumulative regret of MTGD and MPTGD show that multi-start algorithms can further reduce the cumulative regrets.

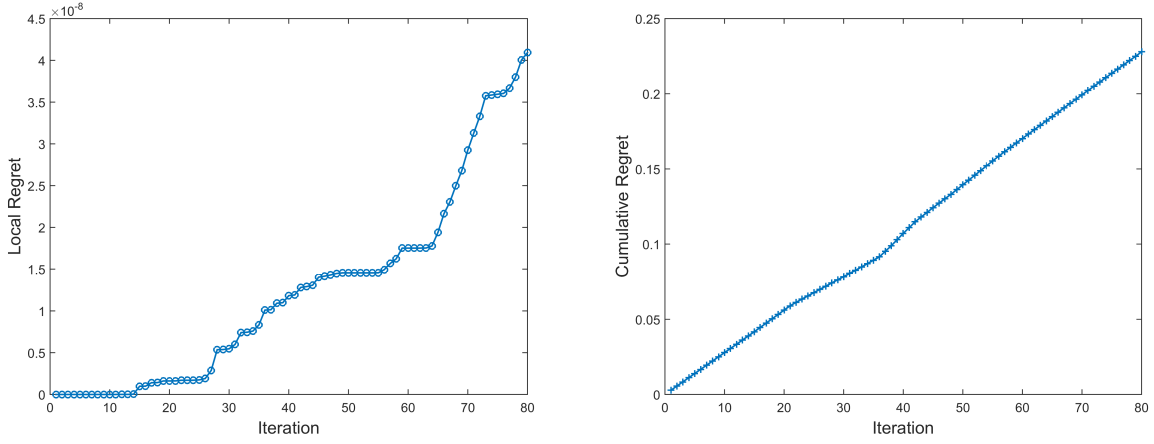


Figure 3: Local regret and Cumulative regret [Hazan et al., 2017, Algorithm 1]

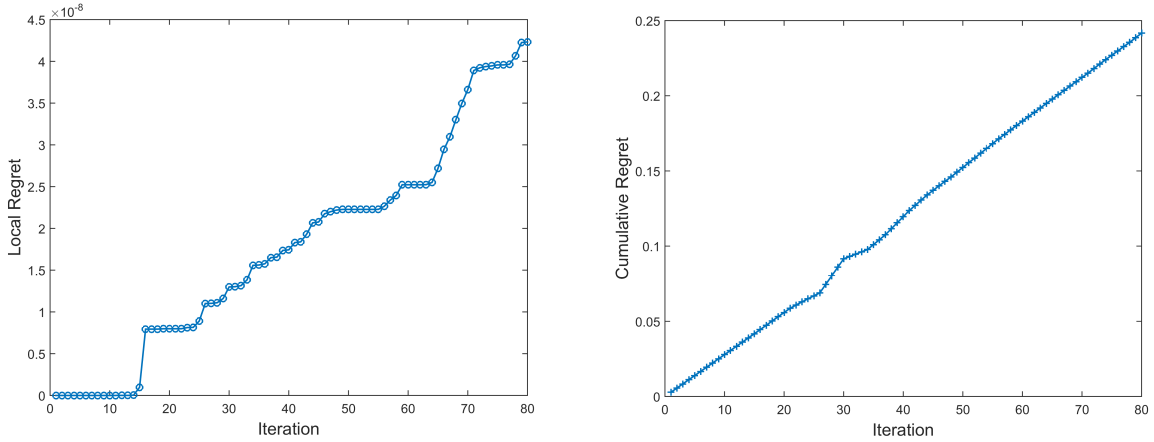


Figure 4: Local regret and Cumulative regret (ATGD)

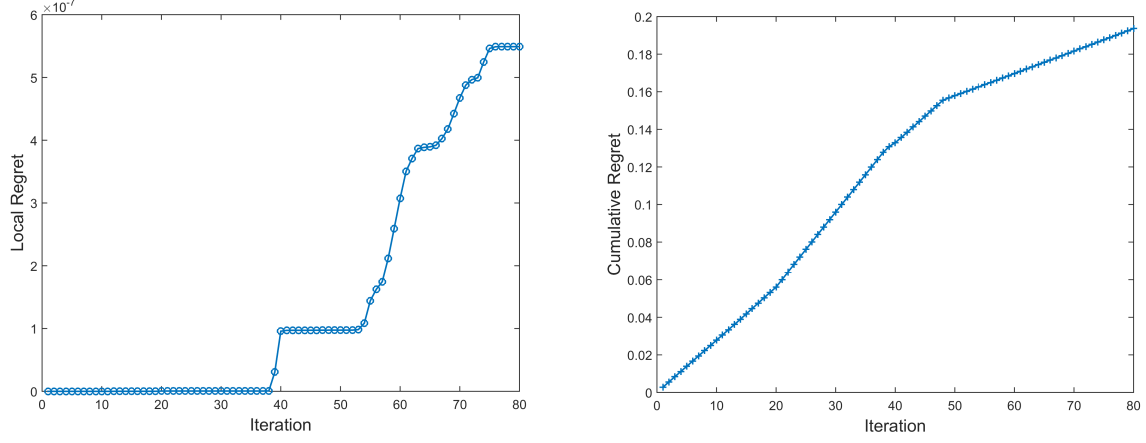


Figure 5: Local regret and Cumulative regret (APTGD)

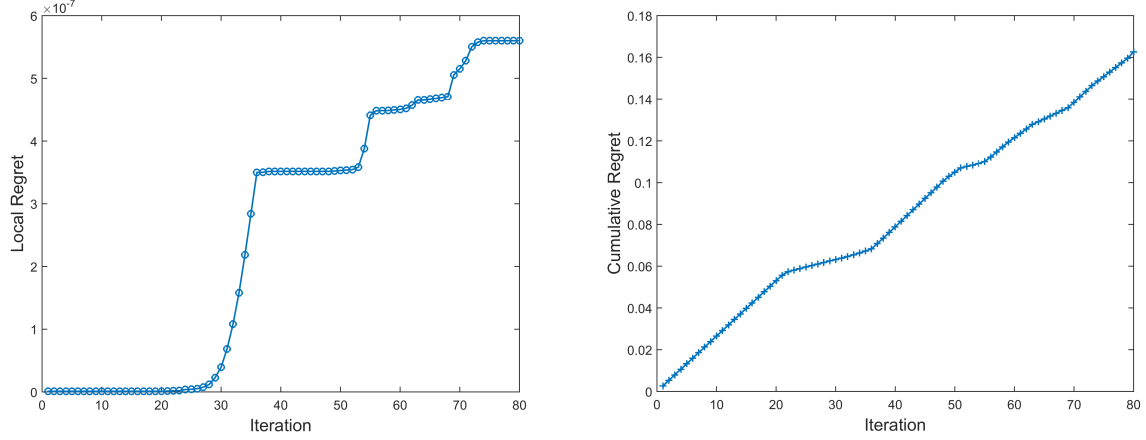


Figure 6: Local regret and Cumulative regret (MTGD)

5.2 Identification Accuracy and Efficiency

In this section, the computational results and the settings for various online algorithms on the real river pollution source identification problem are recorded in Table 1. The contents recorded include the final estimation result for pollution source, the estimation error to the true source information and the average computation time. The initial step-size and the parameters in Backtracking line search are recorded in Table 1. The number of multi-start paths is set to be 30. The result shows that the relative error of estimation on each dimension of ATGD and MTGD is (3.46%, 2.79%, 11.63%). Compared with the estimation result of [Hazan et al., 2017, Algorithm 1] (3.69%, 4.63%, 14.42%), ATGD and MTGD improves the estimation results on every dimension. By incorporating the “escaping from saddle points” module, the error is reduced significantly on the released mass estimation from 3.46% to 1.31%, and the error on the released time estimation is slightly reduced. However, the compensation is that the estimation error on the location estimation is increased to 11.35%. The common shortcoming of [Hazan et al., 2017, Algorithm 1], ATGD, APTGD and MTGD is the high estimation error on the released time estimation. While MPTGD overcomes this shortcoming by reducing the error significantly to 1.40%. MPTGD also costs the highest computation time since both “escaping from saddle points” and multi-start modules are incorporated. [Hazan et al., 2017, Algorithm 1], ATGD, APTGD, MTGD and MPTGD are all conducted under the initial step-sizes

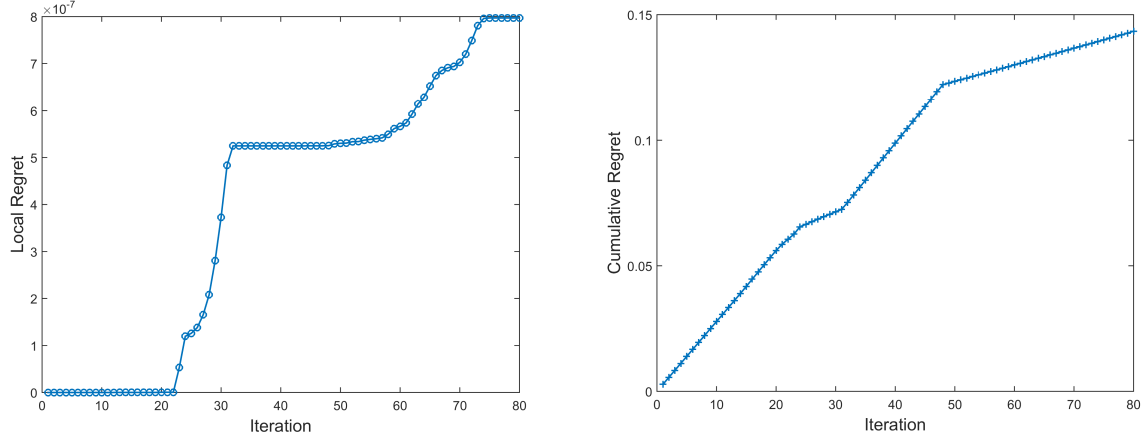


Figure 7: Local regret and Cumulative regret (MPTGD)

$\eta = [110000, 11000000, 75000]$, which is computed based on the method introduced in Section 3.

Although from Table 1, it seems that there does not exist an algorithm in ATGD, APTGD, MTGD and MPTGD that dominates all the others in terms of estimation accuracy in each dimension, the decision-maker could choose to use either of the algorithm based on their own requirement. While for this real-life problem, the decision maker is recommended to use ATGD and MTGD if he has high estimation accuracy requirement on the location estimation, to use APTGD if he has high estimation accuracy requirement on the released mass estimation, and to use MPTGD if he has high estimation accuracy requirement on the released time estimation. Thus, options and guideline for decision maker to choose the proper variant of algorithms are provided when they have emphasis on the identification accuracy on each dimension.

Table 1: Computational Results and Settings

| Algorithms | (s, l, t) | Percentage Error | Parameter Setting | Time (Second) |
|------------|----------------------|-------------------------|----------------------------|---------------|
| Hazan | (1348, -23130, -184) | (3.69%, 4.63%, 14.42%) | $\beta = 0.000008$ | 0.0382 |
| ATGD | (1345, -22722, -190) | (3.46%, 2.79%, 11.63%) | $\beta = 0.000008$ | 0.1023 |
| APTGD | (1317, -19597, -191) | (1.31%, 11.35%, 11.16%) | $\beta = 0.000002$ | 0.7471 |
| MTGD | (1345, -22722, -190) | (3.46%, 2.79%, 11.63%) | $\beta = 0.000008, I = 30$ | 6.0764 |
| MPTGD | (1392, -20994, -212) | (7.00%, 4.78%, 1.40%) | $\beta = 0.000002, I = 30$ | 21.1709 |

6 Conclusion

In this paper, online non-convex learning algorithms for real-time river pollution source identification problem are developed and analyzed. Our basic algorithm has vectorized and adaptive step-sizes such that it ensures high estimation accuracy on dimensions having different magnitude (released mass, location and released time). In addition, the “escaping from saddle points” module is implemented to form the perturbed algorithm in order to further improve the estimation accuracy. Our basic algorithm has local regret $O(N)$, and the perturbed algorithm has local regret $O(N)$ with a high probability. High probability cumulative regret bound $O(N)$ under particular condition on loss functions is also shown.

Our algorithms are implemented on Rhodamine WT dye concentration data from travel time study on the Truckee River between Glenshire Drive near Truckee, Calif. and Mogul, Nev. [Crompton, 2008]. The experiment results validate all our theoretical regret bounds and show that our algorithms are more superior than existing online algorithm on all dimensions (e.g., released mass s , location l and released time t). In addition, the multi-start version of our algorithms are also developed and analyzed; they show that the multi-start module and “escaping from saddle point” module can achieve a significantly low estimation error on certain dimensions (from 3.69% to 1.21% and from 14.42% to 1.40%). Thus, variants of online algorithms are

provided for decision maker to choose and implement, based on their own estimation accuracy requirement.

For future research, observing that estimating the gradients and project gradients will be very computationally demanding especially when the ADE functions are very complicated, one possible solution is to develop “bandit” algorithm. Instead of observing the full information of losses and computing their gradients on the whole domain, only the function value queried by the decision made is observed, and the limited information is used to construct an effective estimation of gradient direction.

References

[Agarwal et al., 2019] Agarwal, N., Gonen, A., and Hazan, E. (2019). Learning in non-convex games with an optimization oracle. In *Conference on Learning Theory*, pages 18–29.

[Agarwal and Niyogi, 2009] Agarwal, S. and Niyogi, P. (2009). Generalization bounds for ranking algorithms via algorithmic stability. *Journal of Machine Learning Research*, 10(Feb):441–474.

[Armijo, 1966] Armijo, L. (1966). Minimization of functions having lipschitz continuous first partial derivatives. *Pacific Journal of mathematics*, 16(1):1–3.

[Burges et al., 2005] Burges, C., Shaked, T., Renshaw, E., Lazier, A., Deeds, M., Hamilton, N., and Hullender, G. (2005). Learning to rank using gradient descent. In *Proceedings of the 22nd international conference on Machine learning*, pages 89–96. ACM.

[Crompton, 2008] Crompton, E. J. (2008). Traveftime for the Truckee River between Tahoe City, California, and Vista, Nevada, 2006 and 2007. USGS Numbered Series 2008-1084, Geological Survey (U.S.).

[De Smedt et al., 2005] De Smedt, F., Brevis, W., and Debels, P. (2005). Analytical solution for solute transport resulting from instantaneous injection in streams with transient storage. *Journal of Hydrology*, 315(1-4):25–39.

[Dennis Jr and Schnabel, 1996] Dennis Jr, J. E. and Schnabel, R. B. (1996). *Numerical methods for unconstrained optimization and nonlinear equations*, volume 16. Siam.

[Drusvyatskiy and Lewis, 2018] Drusvyatskiy, D. and Lewis, A. S. (2018). Error bounds, quadratic growth, and linear convergence of proximal methods. *Math. Oper. Res.*, 43(3):919–948.

[Freund et al., 2003] Freund, Y., Iyer, R., Schapire, R. E., and Singer, Y. (2003). An efficient boosting algorithm for combining preferences. *Journal of machine learning research*, 4(Nov):933–969.

[Gao et al., 2018] Gao, X., Li, X., and Zhang, S. (2018). Online learning with non-convex losses and non-stationary regret. In Storkey, A. J. and Pérez-Cruz, F., editors, *International Conference on Artificial Intelligence and Statistics, AISTATS 2018, 9-11 April 2018, Playa Blanca, Lanzarote, Canary Islands, Spain*, volume 84 of *Proceedings of Machine Learning Research*, pages 235–243. PMLR.

[Ge et al., 2015] Ge, R., Huang, F., Jin, C., and Yuan, Y. (2015). Escaping from saddle points — online stochastic gradient for tensor decomposition.

[Gimbutas and Žilinskas, 2016] Gimbutas, A. and Žilinskas, A. (2016). On global optimization using an estimate of lipschitz constant and simplicial partition. In *AIP Conference Proceedings*, volume 1776, page 060012. AIP Publishing.

[Hazan, 2016] Hazan, E. (2016). Introduction to online convex optimization. *Foundations and Trends in Optimization*, 2(3-4):157–325.

[Hazan et al., 2017] Hazan, E., Singh, K., and Zhang, C. (2017). Efficient regret minimization in non-convex games. In Precup, D. and Teh, Y. W., editors, *Proceedings of the 34th International Conference on Machine Learning, ICML 2017, Sydney, NSW, Australia, 6-11 August 2017*, volume 70 of *Proceedings of Machine Learning Research*, pages 1433–1441. PMLR.

[Hazard et al., 2014] Hazard, A., Giovannelli, J.-F., Dubost, S., and Chatellier, L. (2014). Inverse transport problem of estimating point-like source using a Bayesian parametric method with MCMC. *Signal Processing*, 96(PB):346–361.

[Jha and Datta, 2012] Jha, M. and Datta, B. (2012). Three-dimensional groundwater contamination source identification using adaptive simulated annealing. *Journal of Hydrologic Engineering*, 18(3):307–317.

[Ji et al., 2017] Ji, L., Liu, J., Li, Z., Pan, B., and Sun, M. (2017). Accidents of Water Pollution in China in 2011-2015 and Their Causes. *Journal of Ecology and Rural Environment*, 33(9):775–782.

[Jiang et al., 2017] Jiang, J., Dong, F., Liu, R., and Yuan, Y. (2017). Applicability of Bayesian inference approach for pollution source identification of river chemical spills: A tracer experiment based analysis of algorithmic parameters, impacts and comparison with Frequentist approaches. *China Environmental Science*, 37(10):3813–3825.

[Jiang et al., 2015] Jiang, M., Huang, W., Huang, Z., and Yen, G. G. (2015). Integration of global and local metrics for domain adaptation learning via dimensionality reduction. *IEEE transactions on cybernetics*, 47(1):38–51.

[Jin et al., 2017] Jin, C., Ge, R., Netrapalli, P., Kakade, S. M., and Jordan, M. I. (2017). How to escape saddle points efficiently.

[Levy, 2016] Levy, K. Y. (2016). The power of normalization: Faster evasion of saddle points. *CoRR*, abs/1611.04831.

[Li and Mao, 2011] Li, Z. and Mao, X.-z. (2011). Global multiquadric collocation method for groundwater contaminant source identification. *Environmental Modelling*, page 11.

[Li et al., 2016] Li, Z., Mao, X.-Z., Li, T. S., and Zhang, S. (2016). Estimation of river pollution source using the space-time radial basis collocation method. *Advances in Water Resources*, 88:68–79.

[Maillard and Munos, 2010] Maillard, O. and Munos, R. (2010). Online learning in adversarial lipschitz environments. In Balcázar, J. L., Bonchi, F., Gionis, A., and Sebag, M., editors, *Machine Learning and Knowledge Discovery in Databases, European Conference, ECML PKDD 2010, Barcelona, Spain, September 20-24, 2010, Proceedings, Part II*, volume 6322 of *Lecture Notes in Computer Science*, pages 305–320. Springer.

[Nesterov and Polyak, 2006] Nesterov, Y. and Polyak, B. T. (2006). Cubic regularization of newton method and its global performance. *Mathematical Programming*, 108(1):177–205.

[Nocedal and Wright, 2006] Nocedal, J. and Wright, S. (2006). *Numerical optimization*. Springer Science & Business Media.

[Pintér, 2013] Pintér, J. D. (2013). *Global optimization in action: continuous and Lipschitz optimization: algorithms, implementations and applications*, volume 6. Springer Science & Business Media.

[Preis and Ostfeld, 2006] Preis, A. and Ostfeld, A. (2006). Contamination source identification in water systems: A hybrid model trees–linear programming scheme. *Journal of Water Resources Planning and Management*, 132(4):263–273.

[Sanders et al., 1990] Sanders, L. D., Walsh, R. G., and Loomis, J. B. (1990). Toward empirical estimation of the total value of protecting rivers. *Water Resources Research*, 26(7):1345–1357.

[Sergeyev et al., 2013] Sergeyev, Y. D., Strongin, R. G., and Lera, D. (2013). *Introduction to global optimization exploiting space-filling curves*. Springer Science & Business Media.

[Shalev-Shwartz, 2012] Shalev-Shwartz, S. (2012). Online learning and online convex optimization. *Foundations and Trends in Machine Learning*, 4(2):107–194.

[Shao et al., 2006] Shao, M., Tang, X., Zhang, Y., and Li, W. (2006). City clusters in China: Air and surface water pollution. *Frontiers in Ecology and the Environment*, 4(7):353–361.

[Sohrab, 2014] Sohrab, H. H. (2014). Topology of R and continuity. In *Basic Real Analysis*. Springer.

[Srivastava and Singh, 2014] Srivastava, D. and Singh, R. M. (2014). Breakthrough Curves Characterization and Identification of an Unknown Pollution Source in Groundwater System Using an Artificial Neural Network (ANN). *Environmental Forensics*, 15(2):175–189.

[Suggala and Netrapalli, 2019] Suggala, A. S. and Netrapalli, P. (2019). Online non-convex learning: Following the perturbed leader is optimal. *CoRR*, abs/1903.08110.

[Thibault, 2009] Thibault, H.-L. (2009). Facing water crises and shortages in the Mediterranean. In *Water Scarcity, Land Degradation and Desertification in the Mediterranean Region*, pages 93–100. Springer.

[Van Genuchten, 1982] Van Genuchten, M. T. (1982). *Analytical Solutions of the One-Dimensional Convective-Dispersive Solute Transport Equation*. Number 1661. US Department of Agriculture, Agricultural Research Service.

[Wang et al., 2018] Wang, J., Zhao, J., Lei, X., and Wang, H. (2018). New approach for point pollution source identification in rivers based on the backward probability method. *Environmental Pollution*, 241:759–774.

[Wu et al., 2006] Wu, Q., Ying, Y., and Zhou, D.-X. (2006). Learning rates of least-square regularized regression. *Foundations of Computational Mathematics*, 6(2):171–192.

[Yang et al., 2016] Yang, H., Shao, D., Liu, B., Huang, J., and Ye, X. (2016). Multi-point source identification of sudden water pollution accidents in surface waters based on differential evolution and Metropolis Hastings Markov Chain Monte Carlo. *Stochastic Environmental Research and Risk Assessment*, 30(2):507–522.

[Yang et al., 2018] Yang, L., Deng, L., Hajiesmaili, M. H., Tan, C., and Wong, W. S. (2018). An optimal algorithm for online non-convex learning. *POMACS*, 2(2):25:1–25:25.

[Yang et al., 2017] Yang, L., Tan, C., and Wong, W. S. (2017). Recursive exponential weighting for online non-convex optimization. *CoRR*, abs/1709.04136.

[Zhang et al., 2015] Zhang, L., Yang, T., Jin, R., and Zhou, Z. (2015). Online bandit learning for a special class of non-convex losses. In Bonet, B. and Koenig, S., editors, *Proceedings of the Twenty-Ninth AAAI Conference on Artificial Intelligence, January 25-30, 2015, Austin, Texas, USA.*, pages 3158–3164. AAAI Press.

[Zhang and Xin, 2017] Zhang, S.-p. and Xin, X.-k. (2017). Pollutant source identification model for water pollution incidents in small straight rivers based on genetic algorithm. *Applied Water Science*, 7(4):1955–1963.

Appendix

The supplements of the paper are attached in this section.

A Multi-start Algorithms

In this section, the multi-start version algorithms (Algorithm 4 and Algorithm 5) developed from Algorithm 1 and 3, respectively.

Algorithm 4 Multi-start time-smoothed online gradient descent (MTGD)

Input: window size $w \geq 1$, tolerance $\delta > 0$, constant $W, K > 0$, and a convex set \mathcal{F} and group size I ;

Set $x_1, x_1^{(i)} \in \mathcal{F}$ for $i = 1, \dots, I$ arbitrarily

for $n = 1, \dots, N$ **do**

 Observe the cost function $\Psi_n : \mathcal{F} \rightarrow \mathbb{R}$.

 Compute the initial step-size: $\eta_0 = \mathfrak{S}(F_{n,w}, K)$.

for $i = 1, \dots, I$ **do**

 Initialize $x_{n+1}^{(i)} := x_n^{(i)}$.

 Determine η_n^i using Normalized Backtracking-Armijo line search (Algorithm 2) for $x_{n+1}^{(i)}$.

while $\|\nabla_{\mathcal{F}, \eta_n} F_{n,w}(x_{n+1}^{(i)})\| > \delta$ **do**

 Update $x_{n+1}^{(i)} = x_{n+1}^{(i)} - \eta_n^i \otimes \nabla_{\mathcal{F}, \eta_n} F_{n,w}(x_{n+1}^{(i)})$.

end while

Return $x_{n+1} \in \arg \min_{x \in \{x_{n+1}^{(i)}\}_{i=1, \dots, I}} \sum_{m \in M} \left[\frac{1}{|N_m|} \sum_{n \in N_m} (C(x|l_m, t_m^n) - c_m^n) \right]^2$

end for

Algorithm 5 Multi-start perturbed time-smoothed online gradient descent (MPTGD)

Input: window size $w \geq 1$, constant $c \leq 1$, constant $W, K > 0$, and a convex set \mathcal{F} and group size I ;

Input: $\chi = 3 \max \left\{ \log \left(\frac{d\kappa \Delta f}{c\delta^2 \epsilon} \right), 4 \right\}$, $r = \frac{\sqrt{c}}{\chi^2} \cdot \frac{\delta}{\kappa}$, $g_{\text{thres}} = \frac{\sqrt{c}}{\chi^2} \cdot \delta$, $f_{\text{thres}} = \frac{c}{\chi^3} \sqrt{\frac{\delta^3}{\iota}}$, $t_{\text{thres}} = \lceil \frac{\chi}{c^2} \cdot \frac{\kappa}{\sqrt{\iota} \delta} \rceil$, $t_{\text{noise}} = -t_{\text{thres}} - 1$

Set $x_1, x_1^{(i)} \in \mathcal{F}$ for $i = 1, \dots, I$ arbitrarily

for $n = 1, \dots, N$ **do**

 Observe the cost function $\Psi_n : \mathcal{F} \rightarrow \mathbb{R}$.

 Compute the initial step-size: $\eta_0 = \mathfrak{S}(F_{n,w}, K)$.

 Initialize t_{noise} ;

for $i = 1, \dots, I$ **do**

 Initialize $x_{n+1}^{(i)} := x_n^{(i)}$.

for $t = 0, 1, \dots$ **do**

 Determine η_t using Normalized Backtracking-Armijo line search (Algorithm 2).

 Set $x_{n+1}^{(i), t} = x_n^{(i)}$.

if $\|\nabla_{\mathcal{F}, \eta_t} F_{n,w}(x_{n+1}^{(i), t})\| \leq \delta$ and $t - t_{\text{noise}} > t_{\text{thres}}$ **then**

$t_{\text{noise}} = t$, $\tilde{x}_{n+1}^{(i), t} = x_{n+1}^{(i), t}$, $x_{n+1}^{(i), t} = \tilde{x}_{n+1}^{(i), t} + \omega$, where ω uniformly sampled from $\mathbb{B}_0(r)$.

if $t - t_{\text{noise}} = t_{\text{thres}}$ and $F_{n,w}(x_{n+1}^{(i), t}) - F_{n,w}(x_{n+1}^{(i), t_{\text{noise}}}) > -f_n^{\text{thres}}$ **then**

Return $x_{n+1}^{(i)} = x_{n+1}^{(i), t_{\text{noise}}}$

 Update $x_{n+1}^{(i), t+1} = x_{n+1}^{(i), t} - \eta_t \otimes \nabla_{\mathcal{F}, \eta_t} F_{n,w}(x_{n+1}^{(i), t})$.

end for

end for

Return $x_{n+1} \in \arg \min_{x \in \{x_{n+1}^{(i)}\}_{i=1, \dots, I}} \sum_{m \in M} \left[\frac{1}{|N_m|} \sum_{n \in N_m} (C(x|l_m, t_m^n) - c_m^n) \right]^2$

end for

B Supplements for Section 2

Proposition B.1. *The first and second derivatives of $\tilde{C}_{n,m}$ on the interior of \mathcal{F} are bounded.*

Proof. First prove the boundedness of first derivative of $\tilde{C}_{n,m}(s, l, t)$ on (s, l, t) .

$$\begin{aligned} \frac{\partial \tilde{C}_{n,m}(s, l, t)}{\partial s} &= \frac{1}{A\sqrt{4\pi D(t_m^n - t)}} \exp \left[-\frac{(l_m - l - v(t_m^n - t))^2}{4D(t_m^n - t)} - k(t_m^n - t) \right], \\ \frac{\partial \tilde{C}_{n,m}(s, l, t)}{\partial l} &= \frac{s}{A\sqrt{4\pi D(t_m^n - t)}} \cdot \frac{2(l_m - l - v(t_m^n - t))}{4D(t_m^n - t)} \exp \left[-\frac{(l_m - l - v(t_m^n - t))^2}{4D(t_m^n - t)} - k(t_m^n - t) \right], \\ \frac{\partial \tilde{C}_{n,m}(s, l, t)}{\partial t} &= \frac{4\pi D s}{2A[4\pi D(t_m^n - t)]^{3/2}} \exp \left[-\frac{(l_m - l - v(t_m^n - t))^2}{4D(t_m^n - t)} - k(t_m^n - t) \right] \\ &+ \frac{s}{A\sqrt{4\pi D(t_m^n - t)}} \cdot \left[-\frac{(l_m - l)^2}{4D(t_m^n - t)^2} + \frac{v^2}{4D} + k \right] \exp \left[-\frac{(l_m - l - v(t_m^n - t))^2}{4D(t_m^n - t)} - k(t_m^n - t) \right], \end{aligned}$$

Based on Assumption 2.3 (ii), for any $t \in \mathcal{T}$, set $t_m^n - t \neq 0$. It is then clear that the first derivative of $\tilde{C}_{n,m}(s, l, t)$ is continuous. Recall that the feasible set \mathcal{F} is convex and compact set. By the boundedness of compact sets in a metric space, it can be concluded that the first derivative of $\tilde{C}_{n,m}(s, l, t)$ on (s, l, t) is bounded. Following the same idea, the boundedness of second derivatives of $\tilde{C}_{n,m}$ on the interior of \mathcal{F} can be proved. \square

PROOF OF PROPOSITION 2.5: Recall that $\tilde{C}_{n,m}(s, l, t)$ is lipschitz continuous on the set \mathcal{F} based on Proposition 2.4. Thus, given any $x, x' \in \mathcal{F}$, it can be shown that $\|\tilde{C}_{n,m}(x) - \tilde{C}_{n,m}(x')\| \leq \sigma\|x - x'\|$. As f is also lipschitz continuous, it can be obtained that there exists

$$\|f(\tilde{C}_{n,m}(x)) - f(\tilde{C}_{n,m}(x'))\| \leq \kappa_m \|\tilde{C}_{n,m}(x) - \tilde{C}_{n,m}(x')\|, \forall m \in M.$$

Then, based on the triangle inequality, it can be shown that

$$\begin{aligned} \|\Psi_n(x) - \Psi_n(x')\| &= \left\| \sum_{m \in M} f(\tilde{C}_{n,m}(x)) - \sum_{m \in M} f(\tilde{C}_{n,m}(x')) \right\| \\ &\leq \sum_{m \in M} \|f(\tilde{C}_{n,m}(x)) - f(\tilde{C}_{n,m}(x'))\| \\ &\leq \sum_{m \in M} \kappa_m \|\tilde{C}_{n,m}(x) - \tilde{C}_{n,m}(x')\| \\ &\leq \sum_{m \in M} \kappa_m \sigma \|x - x'\|. \end{aligned}$$

Thus, there exists $\kappa = \sum_{m \in M} \kappa_m \sigma$ such that $\|\Psi_n(x) - \Psi_n(x')\| \leq \kappa \|x - x'\|$. For (ii) Recall that $\nabla_x f$ is lipschitz continuous. For any $x, x' \in \mathcal{F}$,

$$\|\nabla_x f(\tilde{C}_{n,m}(x)) - \nabla_x f(\tilde{C}_{n,m}(x'))\| \leq \kappa_m \|x - x'\|.$$

Based on the triangle inequality, then

$$\|\nabla_x f(\tilde{C}_{n,m}(x))\| \leq \|\nabla_x f(\tilde{C}_{n,m}(x'))\| + \kappa_m \|x - x'\|.$$

Fix the value $x' \in \mathcal{F}$. As the feasible set of \mathcal{F} is a convex and compact set, then $\|\nabla_x(\tilde{C}_{n,m}(x))\|$ is bounded, i.e., there exists $K_{1m} > 0$, such that $\|\nabla_x(\tilde{C}_{n,m}(x))\| \leq K_{1m}$. Besides, based on Proposition 2.4, it can be

shown that, there exists $K_{2m} > 0$ such that $\|\nabla_x \tilde{C}_{n,m}(x')\| \leq K_{2m}$, $\|\nabla_x \tilde{C}_{n,m}(x) - \nabla_x \tilde{C}_{n,m}(x')\| \leq \gamma \|x - x'\|$ and

$$\begin{aligned}
& \|\nabla_x \Psi_n(x) - \nabla_x \Psi_n(x')\| \\
&= \left\| \nabla_x \sum_{m \in M} f(\tilde{C}_{n,m}(x)) - \nabla_x \sum_{m \in M} f(\tilde{C}_{n,m}(x')) \right\| \\
&= \left\| \sum_{m \in M} \nabla_x f(\tilde{C}_{n,m}(x)) \nabla_x \tilde{C}_{n,m}(x) - \sum_{m \in M} \nabla_x f(\tilde{C}_{n,m}(x')) \nabla_x \tilde{C}_{n,m}(x') \right\| \\
&\leq \sum_{m \in M} \|\nabla_x f(\tilde{C}_{n,m}(x)) \nabla_x \tilde{C}_{n,m}(x) - \nabla_x f(\tilde{C}_{n,m}(x')) \nabla_x \tilde{C}_{n,m}(x')\| \\
&= \sum_{m \in M} \|\nabla_x f(\tilde{C}_{n,m}(x)) \nabla_x \tilde{C}_{n,m}(x) - \nabla_x f(\tilde{C}_{n,m}(x)) \nabla_x \tilde{C}_{n,m}(x') \\
&\quad + \nabla_x f(\tilde{C}_{n,m}(x)) \nabla_x \tilde{C}_{n,m}(x') - \nabla_x f(\tilde{C}_{n,m}(x')) \nabla_x \tilde{C}_{n,m}(x')\| \\
&\leq \sum_{m \in M} \|\nabla_x f(\tilde{C}_{n,m}(x))\| \|\nabla_x \tilde{C}_{n,m}(x) - \nabla_x \tilde{C}_{n,m}(x')\| \\
&\quad + \sum_{m \in M} \|\nabla_x \tilde{C}_{n,m}(x')\| \|\nabla_x f(\tilde{C}_{n,m}(x)) - \nabla_x f(\tilde{C}_{n,m}(x'))\| \\
&\leq \sum_{m \in M} (K_{1m} \gamma + K_{2m} \kappa_m) \|x - x'\|.
\end{aligned}$$

Let $\beta = \sum_{m \in M} (K_{1m} \gamma + K_{2m} \kappa_m)$. Thus, it can be concluded that there exists β such that

$$\|\nabla_x \Psi_n(x) - \nabla_x \Psi_n(x')\| \leq \beta \|x - x'\|.$$

For (iii), Given the results in (ii) and implement the same arguments in (ii) with Definition 2.1, the desired results are derived.

PROOF OF PROPOSITION 2.8: See [Hazan et al., 2017, Proposition 2.4]. Let $u := x + \eta \otimes \nabla \Psi(x)$, and $v := u + \eta \otimes \nabla \Phi(x)$. Define their respective projection $u' = \Pi_{\mathcal{F}}[u]$, and $v' = \Pi_{\mathcal{F}}[v]$, so that $u' = x - \eta \otimes \nabla_{\mathcal{F}, \eta} \Psi(x)$, and $v' = x - \eta \otimes \nabla_{\mathcal{F}, \eta} [\Psi + \Phi](x)$. It can be first shown that $\|u' - v'\| \leq \|u - v\|$.

By the generalized Pythagorean theorem for convex sets, both $\langle (u' - v') \otimes \eta, (v - v') \otimes \eta \rangle \leq 0$ and $\langle (v' - u') \otimes \eta, (u - u') \otimes \eta \rangle \leq 0$ are derived. Summing these, it can be shown

$$\begin{aligned}
& \langle (u' - v') \otimes \eta, [u' - v' - (u - v)] \otimes \eta \rangle \leq 0 \\
& \implies \|(u' - v') \otimes \eta\|^2 \leq \langle (u' - v') \otimes \eta, (u - v) \otimes \eta \rangle \\
& \leq \|(u' - v') \otimes \eta\| \cdot \|(u - v) \otimes \eta\|,
\end{aligned}$$

as claimed. Finally, by the triangle inequality,

$$\begin{aligned}
& \|\nabla_{\mathcal{F}, \eta} [\Psi + \Phi](x)\| - \|\nabla_{\mathcal{F}, \eta} \Psi(x)\| \\
& \leq \|\nabla_{\mathcal{F}, \eta} [\Psi + \Phi](x) - \nabla_{\mathcal{F}, \eta} \Psi(x)\| \\
& = \|(u' - v') \otimes \eta\| \\
& \leq \|(u - v) \otimes \eta\| \\
& = \|\nabla \Phi(x)\|,
\end{aligned}$$

as required.

C Supplements for Section 3

PROOF OF THEOREM 3.3: Let us start to prove Theorem 3.3 (i) by the following statement. Given η_n computed from Algorithm 2, it can be verified that for all $x \in \mathcal{F}$, and $n \geq 2$, that

$$\|\nabla_{\mathcal{F}, \eta_0} F_{n-1, w}(x)\|_2^2 \leq \|\nabla_{\mathcal{F}, \eta_n} F_{n-1, w}(x)\|_2^2. \quad (\text{C.1})$$

The above equality holds based on the definition of projected gradient as well as the fact that $\eta_n \leq \eta_0$. Note Algorithm 1 only play an iterate x_n if $\|\nabla_{\mathcal{F}, \eta_n} F_{n-1, w}(x_n)\|_2^2 \leq \delta/w$. (Note that $n = 1$, $F_{n-1, w}$ is zero.) Let $h_n(x) = \frac{1}{w} [\Psi_n(x) - \Psi_{n-w}(x)]$, which is $\frac{2\kappa}{w}$ -Lipschitz. Then, for each $1 \leq n \leq N$,

$$\begin{aligned} \|\nabla_{\mathcal{F}, \eta_0} F_{n, w}(x_n)\|_2^2 &= \|\nabla_{\mathcal{F}, \eta_0} [F_{n-1, w} + h_n](x_n)\|_2^2 \\ &\leq \|\nabla_{\mathcal{F}, \eta_0} F_{n-1, w}(x_n)\|_2^2 + \|\nabla h_n(x_n)\|_2^2 \\ &\leq \|\nabla_{\mathcal{F}, \eta_n} F_{n-1, w}(x_n)\|_2^2 + \|\nabla h_n(x_n)\|_2^2 \\ &\leq (\delta + \frac{2\kappa}{w})^2. \end{aligned}$$

for any $x \in \mathcal{F}$. The last equality holds based on equality (C.1), Proposition 2.8 as well as the stopping criterion of ATGD (Algorithm 1).

To prove Theorem 3.3 (ii), the following lemmas are introduced.

Lemma C.1. *Let \mathcal{F} be a closed convex set, and let $\eta \in \mathbb{R}_+^d$. Suppose $\Psi: \mathcal{F} \rightarrow \mathbb{R}$ is differentiable. Then for any $x \in \mathbb{R}$,*

$$\langle \nabla \Psi(x), \eta^2 \otimes \nabla_{\mathcal{F}, \eta} \Psi(x) \rangle \geq \|\eta \otimes \nabla_{\mathcal{F}, \eta} \Psi(x)\|_2^2.$$

Proof. Let $u = x - \eta \otimes \nabla \Psi(x)$, and $u' = \Pi_{\mathcal{F}}[u]$. Then

$$\begin{aligned} &\langle -\eta \otimes \nabla \Psi(x), -\eta \otimes \nabla_{\mathcal{F}, \eta} \Psi(x) \rangle - \|\eta \otimes \nabla_{\mathcal{F}, \eta} \Psi(x)\|_2^2 \\ &= \langle u - x, u' - x \rangle - \langle u' - x, u' - x \rangle \\ &= \langle u - u', u' - x \rangle \geq 0, \end{aligned}$$

where the last inequality follows by the generalized Pythagorean theorem. \square

For $2 \leq n \leq N$, let τ_n be the number of gradient steps taken in the outer loop at iteration $n-1$, in order to compute the iterate x_n . For convenience, define $\tau_1 = 0$. A progress lemma during each gradient descent epoch is established:

Lemma C.2. *For any $2 \leq n \leq N$, there exists $\eta' \leq \eta_0$ such that*

$$F_{n-1, w}(x_n) - F_{n-1, w}(x_{n-1}) \leq -\tau_n \left(\|\eta'\|_{\min} - \frac{\beta \|\eta_0\|_{\infty}^2}{2} \right) \delta^2.$$

Proof. Consider a single iterate z of the loop of n , and the next iterate $z' := z - \eta_n \otimes \nabla_{\mathcal{F}, \eta_n} F_{n-1, w}(z)$ when the step-size is η_n . It can be shown by the β -smoothness of $F_{n-1, w}$,

$$\begin{aligned} F_{n-1, w}(z') - F_{n-1, w}(z) &\leq \langle \nabla F_{n-1, w}(z), z' - z \rangle + \frac{\beta}{2} \|z' - z\|_2^2 \\ &= -\langle \nabla F_{n-1, w}(z), \eta_n \otimes \nabla_{\mathcal{F}, \eta_n} F_{n-1, w}(z) \rangle + \frac{\beta}{2} \|\eta_n \otimes \nabla_{\mathcal{F}, \eta_n} F_{n-1, w}(z)\|_2^2 \\ &\leq -\|\eta_n\|_{\min} \|\nabla_{\mathcal{F}, \eta_n} F_{n-1, w}(z)\|_2^2 + \frac{\beta}{2} \|\eta_n \otimes \nabla_{\mathcal{F}, \eta_n} F_{n-1, w}(z)\|_2^2 \\ &\leq -\left(\|\eta'\|_{\min} - \frac{\beta \|\eta_0\|_{\infty}^2}{2} \right) \|\nabla_{\mathcal{F}, \eta_n} F_{n-1, w}(z)\|_2^2. \end{aligned}$$

\square

The last equality holds when choosing $\eta' \leq \eta_t$. The algorithm only takes projected gradient steps when $\|\nabla_{\mathcal{F}, \eta_t} F_{n-1, w}(z)\| \geq \delta$. Summing across all τ_n consecutive iterations in the epoch yields the claim.

To complete the proof of the theorem, write the telescopic sum:

$$\begin{aligned}
F_{N,w}(x_N) &= \sum_{n=1}^N [F_{n,w}(x_n) - F_{n-1,w}(x_{n-1})] \\
&= \sum_{n=1}^N [F_{n-1,w}(x_n) - F_{n-1,w}(x_{n-1}) + f_{n,w}(x_n) - f_{n-w,w}(x_n)] \\
&\leq \sum_{n=2}^N [F_{n-1,w}(x_n) - F_{n-1,w}(x_{n-1})] + \frac{2BN}{w}.
\end{aligned}$$

Using Lemma C.2,

$$F_{N,w}(x_N) \leq \frac{2BN}{w} - \left(\|\eta'\|_{\min} - \frac{\beta \|\eta_0\|_\infty^2}{2} \right) \delta^2 \cdot \sum_{n=1}^N \tau_n,$$

hence

$$\begin{aligned}
\sum_{n=1}^N \tau_n &\leq \frac{1}{\delta^2 \left(\|\eta'\|_{\min} - \frac{\beta \|\eta_0\|_\infty^2}{2} \right)} \cdot \left(\frac{2BN}{w} - F_{N,w}(x_N) \right) \\
&\leq \frac{2B}{\delta^2 \left(\|\eta'\|_{\min} - \frac{\beta \|\eta_0\|_\infty^2}{2} \right) w} N,
\end{aligned}$$

as claimed.

D Supplements for Section 4

PROOF OF THEOREM 4.2: Recall that an $\tilde{\epsilon}$ -second order stationary is point with a small gradient, and where the Hessian does not have a significant negative eigenvalue. Suppose currently at an iterate x_t that is not an $\tilde{\epsilon}$ -second-order stationary point, there are two possibilities:

1. Gradient is large: $\|\nabla_x \Psi_n(x_n^t)\|_2 \geq g_{\text{thres}}$, or
2. Around saddle point: $\|\nabla_x \Psi_n(x_n^t)\|_2 \leq g_{\text{thres}}$ and $\lambda_{\min}(\nabla_x^2 \Psi_n(x_n^t)) \leq \sqrt{\iota\tilde{\epsilon}}$.

The following two lemmas address the above two possibility respectively, which guarantee that perturbed gradient descent will decrease the function value in both scenarios. Next lemma shows if the current gradient is large, progress is made in function value in proportion of the square of norm of the gradient.

Lemma D.1. *Assume that Ψ_n satisfies the condition in Proposition 2.5. Then for gradient decent with step-size $\|\eta\|_\infty \leq 1/\kappa$, there exists $\eta' \leq \eta$,*

$$\Psi_n(x_n^{t+1}) \leq \Psi_n(x_n^t) - \left(\|\eta'\|_{\min} - \frac{\|\eta_0\|_\infty}{2} \right) \|\nabla_x \Psi_n(x_n^t)\|_2^2.$$

Proof. By the properties in Proposition 2.5,

$$\begin{aligned}
\Psi_n(x_n^{t+1}) &\leq \Psi_n(x_n^t) + \nabla_x \Psi_n(x_n^t)^\top (x_n^{t+1} - x_n^t) + \frac{\kappa}{2} \|x_n^{t+1} - x_n^t\|_2^2 \\
&\leq \Psi_n(x_n^t) - \|\eta_t\|_{\min} \|\nabla_x \Psi_n(x_n^t)\|_2^2 + \frac{\kappa \|\eta_t\|_\infty^2}{2} \|\nabla_x \Psi_n(x_n^t)\|_2^2 \\
&\leq \Psi_n(x_n^t) - \left(\|\eta'\|_{\min} - \frac{\|\eta_0\|_\infty}{2} \right) \|\nabla_x \Psi_n(x_n^t)\|_2^2
\end{aligned}$$

□

The next lemma shows a perturbation followed by a small number of standard gradient descent steps can also make the function value decrease with high probability.

Lemma D.2. *There exists an absolute constant c_{max} , for Ψ_n satisfies properties in Proposition 2.5 and 4.1, and any $c \leq c_{max}$, and $\chi \geq 1$. Let $\eta_0, r, g_{thres}, f_{thres}, t_{thres}$ computed as Algorithm 3. Then if \tilde{x}_n^t satisfies:*

$$\|\nabla_x \Psi_n(\tilde{x}_n^t)\|_2 \leq g_{thres}, \quad \text{and} \quad \lambda_{\min}(\nabla_x^2 \Psi_n(\tilde{x}_n^t)) \geq -\sqrt{\iota \tilde{\epsilon}}.$$

Let $x_n^t = \tilde{x}_n^t + \omega_t$ where ω_t comes from the uniform distribution over $\mathbb{B}_0(r)$ and let x_n^{t+1} be the iterates of gradient descent from x_n^t with step-size η_t , then with at least probability $1 - \frac{d\kappa}{\sqrt{\iota\epsilon}} \exp(-\chi)$,

$$\Psi_n(x_n^{t+t_{thres}}) - \Psi_n(\tilde{x}_n^t) \leq -f_{thres}.$$

In [Jin et al., 2017, Section 5.2] and [Jin et al., 2017, Section A.2], detailed proofs have been derived for fixed step-size version of Lemma D.2. The main idea is listed as follows. After adding a perturbation, the current point of the algorithm comes from a uniform distribution over a d -dimensional ball centered at \tilde{x}_n^t . This perturbation ball can be divided into two adjoint regions: (1) an *escaping* region which consists of all the points whose function value decrease by a least f_{thres} after t_{thres} steps; (2) a *stuck* region. The proof is to show that the stuck region only consists of a very small proportion of the volume of perturbation ball and the current point has very small chance of falling in the stuck region. The proofs of Lemma D.2 will still hold for vectorized and adjusted step-size η_t , since $\eta_t \leq \eta_0$ (see [Jin et al., 2017, Lemma 14, 15, 16 and 17]).

To prove Theorem 4.2 following [Jin et al., 2017, Appendix A], suppose in epoch n , the point x_0 will be the start point that $\|\nabla_x \Psi_n(x_0)\|_2 \leq g_{thres}$. Then Algorithm 3 will add perturbation and check the termination condition. If the condition is not met, it must follow that

$$f(x_{thres}) - f(x_0) \leq -f_{thres} = -\frac{c}{\chi^3} \cdot \sqrt{\frac{\delta^3}{\iota}}.$$

This means on average every step decreases the function value by

$$\frac{f(x_{thres}) - f(x_0)}{t_{thres}} \leq -\frac{c^3}{\chi^4} \cdot \frac{\delta^2}{\iota},$$

which further means that in each epoch n , Algorithm 3 will terminate within the following number of iterations:

$$\frac{\Delta f}{\frac{c^3}{\chi^4} \cdot \frac{\delta^2}{\iota}} = \frac{\chi^4}{c^3} \cdot \frac{\iota \Delta f}{\delta^2} = O\left(\frac{\iota \Delta f}{\delta^2} \log^4\left(\frac{d \iota \Delta f}{\delta^2 \epsilon}\right)\right).$$

It can also be shown that in each epoch when Algorithm 3 terminates, the point it finds is actually an δ -second-order stationary point of $F_{n,w}$. On the other hand, during the entire run of Algorithm 3 in each epoch, the number of times the perturbations are added, is at most:

$$\frac{1}{t_{thres}} \cdot \frac{\chi^4}{c^3} \cdot \frac{\iota \Delta f}{\delta^2} = \frac{\chi^3}{c} \frac{\sqrt{\iota \delta \Delta f}}{\delta^3}.$$

Finally if Algorithm 3 works correctly, the probability of that is at least

$$1 - \frac{d\kappa}{\sqrt{\iota\epsilon}} \exp(-\chi) \frac{\chi^3}{c} \frac{\sqrt{\iota \delta \Delta f}}{\delta^3} \geq 1 - \delta,$$

given the formulation of χ .

ILLUSTRATION OF EXAMPLE 4.4 : Choose Least square loss and recall the function:

$$\Psi_n(x) = \sum_{m \in M} (\tilde{C}_{n,m}(x))^2.$$

In the ζ -domain of x_N^* ,

$$\begin{aligned}
& \frac{1}{N} \sum_{n=1}^N \Psi_n(x_N^*) - \frac{1}{N} \sum_{n=1}^N \Psi_n(x) \\
& \geq \frac{2}{N} \sum_{n=1}^N \sum_{m \in M} [\tilde{C}_{n,m}(x) (\tilde{C}_{n,m}(x_N^*) - \tilde{C}_{n,m}(x)) + \|\tilde{C}_{n,m}(x_N^*) - \tilde{C}_{n,m}(x)\|^2] \\
& \geq \frac{2}{N} \sum_{n=1}^N \sum_{m \in M} [\tilde{C}_{n,m}(x) \nabla \tilde{C}_{n,m}(x) (x_N^* - x) + \sigma' \|x_N^* - x\|^2],
\end{aligned}$$

where the first inequality holds based on the strongly convexity of Least square loss, and the second inequality holds based on the two conditions in Example 4.4. Thus it can be shown that function $\frac{1}{N} \sum_{n=1}^N \Psi_n(x)$ is $2\sigma' |M|$ -strongly convex on the ζ -domain of x_N^* . Then based on Polyak-Lojasiewicz inequalities, the desired results are gained. In the ζ -domain of $x^{n,*}$ for all $n \leq N$, the same statement can be used to show the strongly convexity of function $\Psi_n(x)$, for all $n \leq N$.

PROOF OF THEOREM 4.5: With probability $1 - \epsilon$, and after $O\left(\frac{\kappa \Delta f w^2}{\delta^2} \log^4\left(\frac{d\kappa \Delta f w^2}{\delta^2 \epsilon}\right) N\right)$ gradient estimations, the average cumulative regret denoted by \mathfrak{R}_G until time N is,

$$\begin{aligned}
\frac{\mathfrak{R}_G(N)}{N} &= \frac{1}{N} \left[\sum_{n=1}^N \Psi_n(x_n) - \inf_{x \in \mathcal{F}} \sum_{n=1}^N \Psi_n(x) \right] \\
&\leq \frac{1}{N} \left[\sum_{n=1}^N \Psi_n(x_n) - \sum_{n=1}^N \Psi_n(x^{n,*}) \right] + \frac{1}{N} \sum_{n=1}^N \Psi_n(x_n) - \frac{1}{N} \sum_{n=1}^N \Psi_n(x_N^*) \\
&\leq \frac{\delta + 2\kappa}{\mu N} + \frac{\delta + 2\kappa}{\mu},
\end{aligned}$$

where the first inequality holds since $\Psi_n(x_n) \geq \Psi_n(x^{n,*})$ for all $1 \leq n \leq N$ and the second inequality holds based on the condition in Definition 4.3.